RESEARCH STUDY ON HYDROGEN THYRATRONS

Sixth Quarterly Progress Report

Period Covered: 15 October 1952 to 15 January 1953

Signal Corps Contract Number DA36-039 sc-15372

Department of the Army Project Number 3-19-02-031

Signal Corps Project Number 27-313A

Placed By: United States Army
Signal Corps Procurement Agency
Laboratory Office
Fort Monmouth, New Jersey

Contractor: Edgerton, Germeshausen & Grier, Inc.
160 Brookline Avenue
Boston 15, Massachusetts

Research Study on Hydrogen Thyratrons

Sixth Quarterly Progress Report

Period Covered: 15 October 1952 - 15 January 1953

The object of this research is to conduct investigations directed toward fulfilling the requirements of Signal Corps Technical Requirements Number SCL-2471, dated 5 March 1951, entitled, "Basic Investigation of Hydrogen Thyratrons".

Signal Corps Contract Number DA36-039 sc-15372

Signal Corps Technical Requirement Number SCL-2471, 5 March 1951

Department of the Army Project Number 3-19-02-031

Signal Corps Project Number 27-313A

Report Prepared by: Stuart T. Martin
Seymour Goldberg

Report Approved by: K. J. Germeshausen
Vice-President

TABLE OF CONTENTS

PURPOSE

It is the purpose of this contract to determine the fundamental design parameters of hydrogen thyratrons. This task is being accomplished by measurement of existing thyratrons, together with a study of their fundamental processes, in order to determine their limitations. As a final step the development of an improved thyratron will be undertaken.

The work is being undertaken in four more or less distinct phases. These are:

a) A determination of the effect of various conditions of operation on tube life.

b) A program of research, both experimental and theoretical, to determine the basic characteristics of the discharge as they affect the operation of the thyratron.

c) A study of the causes of hydrogen loss from thyratrons.

d) Design and fabrication of a thyratron of improved performance.

Life tests are being conducted on lots of twelve 4C35's simultaneously in order that individual tests will have some statistical significance. These tests receive guidance from the experimental and theoretical research. In order to obtain reliable information in the most effective manner, initial results obtained on the smaller tubes will be extended by scaling on smaller lots of a larger tube. The 1907 has been selected for this purpose.

Experimental and theoretical research is being conducted to discover the properties of an electrical discharge in hydrogen which are important to thyratron operation. These include the mechanism of break-

down and recovery and the properties of the discharge during the steady state conduction of high currents.

The purpose of the final phase, to design and fabricate a thyratron of improved ratings, is primarily to prove out design parameters and materials resulting from earlier work. It may become necessary in the course of this work to undertake a further study of hydrogen generation.

ABSTRACT

Results of life test at 5600 pulses per second and 8000 pulses per second are presented. In these tests the P_B factor has been increased over the JAN value, but average and peak powers have been kept constant. The effect of inverse voltage has been shown to be of great importance to life at high repetition rates. Autopsies of tubes completing life are shown and related to performance during life.

Power dissipation at the anode caused by flow of positive ions in the first 100 millimicroseconds after cessation of forward current is responsible for the effect of inverse voltage on life. The details of the appearance of inverse voltage have been analyzed and shown to be in accordance with those experimentally observed.

A life test rack for the 1907 has been completed. A successful oil-cooled load has been designed which minimized inductive effects, and also an improved current viewing resistor having an inductance less than 10^{-9} henrys.

A preliminary design for a ceramic envelope hydrogen thyratron has been made. The details are presented.

FACTUAL DATA

During the past quarter a series of life tests have been run at the 4C35 level designed to increase the P_B factor (e_{py} x p.r.r. x i_b) by increasing the pulse repetition rate. At the same time average current was maintained constant by reducing the pulse length as the frequency increased. In this way the effects of phenomena occuring at the start and end of the pulse could be emphasized. In the course of these investigations it has been discovered that the inverse voltage appearing across the tube in the first fifty to one hundred millimicroseconds after forward current has ceased has an important bearing on anode dissipation and tube life.

The first experiment consisted of running a group of eight tubes at 5600 pulses per second and $\frac{1}{4}$ microsecond pulse length, keeping all other variables constant, by the simple expedient of using only two sections of the four section pulse network used for the JAN life tests (2800 pulses/sec, $\frac{1}{2}$ microsecond). This test, in effect, doubled the P_B factor over the JAN test (2×10^9 JAN compared to 4×10^9). The average life of eight tubes was 1500 hours, significantly less than that reported for the JAN test, 2300 hours. However, autopsy showed that the primary cause of failure was the same in the two cases, namely complete exhaustion of the cathode material. This may be seen in Fig.1 (a) and (b) where the cathode cylinder is quite bare and shiny and there is the heavy film of oxide and nickel curling away from the inner heat shield typical of cathode exhaustion observed on the JAN tests. This separation of the evaporated material from the base apparently does not take place until a cut is made in the heat shield. The underside of the grid

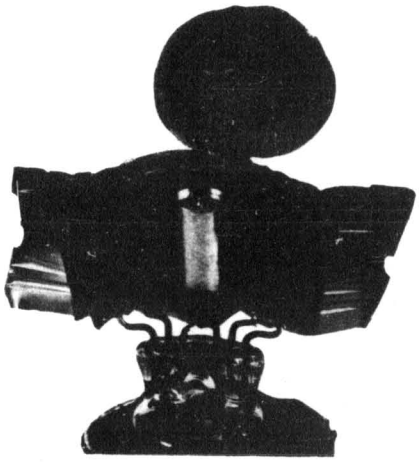

(a) Tube #1736
5600 pps - 1/4 μsec
Inverse 3160V
Life 1639 Hours

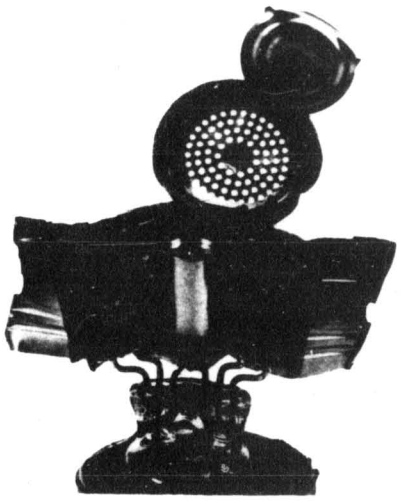

(b) Tube #1736
5600 pps - 1/4 μsec
Inverse 3160V
Life 1639 Hours

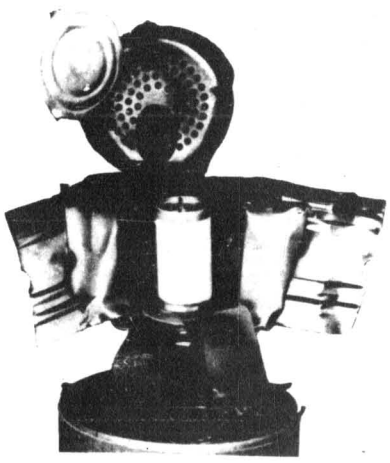

(c) Tube #2597
8000 pps - 1/8 μsec
Inverse 4140V
Life 200 Hours

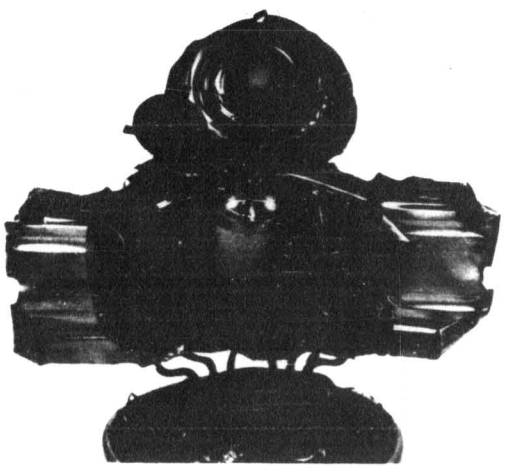

(d) Tube #2817
8000 pps - 1/8 μsec
Inverse 1590V
Opened at 200 Hours

Fig. 1 Autopsy performed on 4C35 Thyratrons.

baffle is covered with a very heavy deposit of cathode material.

Inspection of the operating parameters shown in Figs. 29 a to h show nearly typical behavior for this type of failure. The emission drop has passed through a well defined minimum and risen to quite high values. Correspondingly the cathode temperature at end of life was seen to be quite high.

While this behavior corresponds exactly to that observed in the JAN life tests, three new features have been observed. One is that in every tube except one the grid baffle has been severely bent in one place as seen in Fig. 1 (a) and (b). The material of this part is quite stiff when cold, yet the bent portion forms an angle of nearly 90°. It must have been quite hot for this to happen. In one tube, in fact, this portion of the grid baffle was observed to be at a bright red heat, (at least 800°C) at one point near the end of its life. Another different feature was the observation of red anodes, which also occurred in seven of the eight cases at roughly one-half to three-quarters of the way through life. The last difference was that the symptom at end of life was not usually failure to trigger as observed in the JAN tests, but going into continuous conduction, always associated with signs of grid emission. It may be seen from Figs. 29 that grid currents became appreciable somewhat earlier than in the JAN tests.

From this collection of symptoms it appears that while the primary cause of failure was loss of cathode coating, the immediate effect was associated with the increased power dissipated by the cathode as a result. We may suppose that the grid temperature at which important grid emission will take place is quite critical, particularly as the grid becomes coated with cathode material. The grid receives power from

three sources; the anode, the gas and the cathode. The anode is observed to become red sometime before failure occurs, thus the grid dissipation must be above normal during the latter part of life. The sharply rising emission drop is always associated with a substantial increase in cathode and cathode heat shield temperature. Indeed, at this stage they are both receiving substantial power from the discharge. The combination may well cause the temperature of the grid to rise above safe limits. This will not account for the observation that a portion of the grid baffle has been seen to run red hot in the region where the discharge concentrates, during the latter stages of life. It seems unlikely that there could be enough power in the "trigger" for this to happen and we are left with the possibility that the recombination of ions or of atomic hydrogen is responsible.

Following these tests another group of nine tubes was run at 8000 cycles and 1/8μsec pulse length. This corresponds to a P_B factor of 5.8×10^9, or nearly three times the JAN limit. This time the average life was just 207 hours. Autopsy showed, however, that failure was from a completely different cause. As may be seen in Fig. 1 (c) the cathode coating is quite intact and little material has evaporated to other surfaces. Correspondingly, the emission drop was observed to be still falling at the end of life.

In each case the anode was observed to run at a red heat starting within 50 hours of the beginning of the life test. This heating became progressively more severe during life and it was observed that a combination of expansion of the anode supporting lead and buckling of the grid caused these two surfaces to approach more and more closely. Grid current increased continuously throughout life and eventually the

tube failed because of continuous conduction in many cases. This was obviously caused by the very close approach of grid and anode surfaces.

In conducting this life test the short pulses were produced by reducing the original four-section network to a single section which has a different relationship among the quantities, characteristic impedance, rate of rise of current, inverse voltage and so forth, than a multi-section network that can be approximated by a transmission line. As a result, this test had been run with an inverse voltage between four and five thousand volts instead of between two and three thousand volts as was characteristic of the preceding tests. By experimenting it was found that reducing this inverse to the neighborhood of 1,500 volts substantially reduced the anode heating even though rate of rise of current, pulse length, repetition frequency and all were kept the same. Accordingly, a further test was run with a total of eight tubes at the new condition in which the P_B factor was identical with that of the preceding test but the inverse voltage was approximately one-third (1500 volts).

Under these conditions the average life was 527 hours. Autopsy displayed in Fig.1 (d) indicates again that the catnode is practically intact; failure was from continuous conduction caused by grid emission. Red anodes developed on all of these tubes, usually at about 300 hours and in general became worse as life progressed. Thus, comparing these results and observations with those of the preceding test it was apparent that reduction of the inverse voltage had substantially increased the life under conditions where cathode depletion is not the major cause of failure.

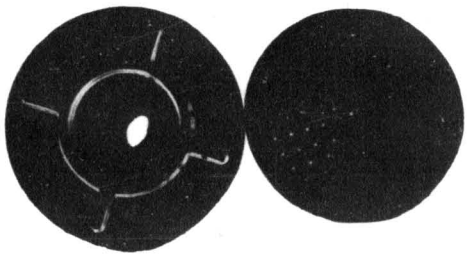

(a) Tube #2597 Life 200 Hours
8000 pps - 1/8 μ sec
Inverse 4140V

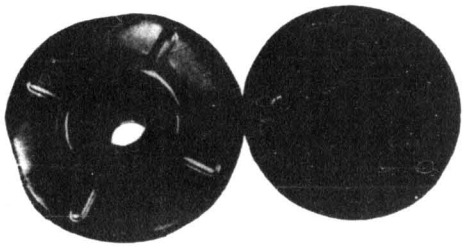

(b) Tube #2817 Life 200 Hours
8000 pps - 1/8 μ sec
Inverse 1590V

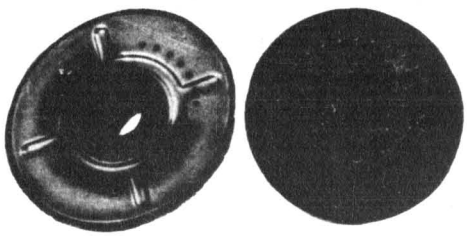

(c) Tube #1736 Life 1639 Hours
5600 pps - 1/4 μ sec
Inverse 3160V

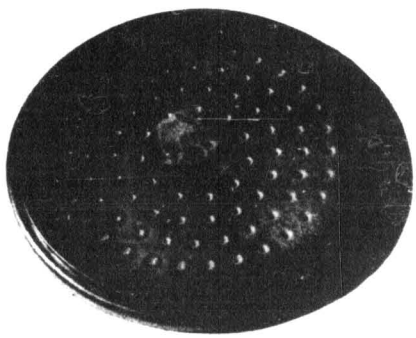

(d) Tube #2875 Life 98 Hours
8000 pps - 1/8 μ sec
Inverse 4160V

Fig. 2 Anodes taken from 4C35 Thyratrons.

Figure 2 compares anodes taken from these three tests; namely, $\frac{1}{4}$ microsecond, 5600 cycles; 1/8 microsecond, 8000 cycles; and two different inverse voltages.

Figure 2 (a) shows the anode and the portion of the grid directly behind it from Tube 2597 which ran 200 hours at 8000 pulses per second and 1/8 microsecond pulse length. On this particular tube the peak inverse voltage, which will be discussed later, was approximately 4000 volts. It will be observed that very severe erosion of the anode has taken place in a manner described in the last quarterly report. However, in this case it is so severe that many holes have been drilled through the molybdenum anode. This anode is approximately 0.020" thick. Adjacent to it is shown the top plate of the grid which is approximately $1\frac{1}{2}$ mm away from the back surface of the anode, parallel to it as shown in Fig. 3 . It will be observed that there is severe pit-

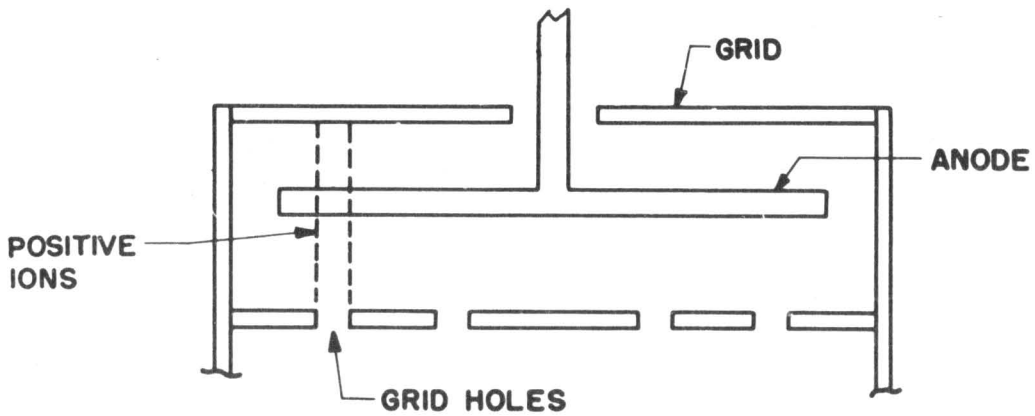

Fig. 3 Schematic diagram of the grid-anode region.

ting of this portion of the tube corresponding to the holes drilled in the anode itself. Figure 2 (b) shows an anode and the corresponding portion of the grid taken from a tube run under identical conditions except that the inverse voltage was approximately 1600 volts. It is ap-

parent that the pitting is much less severe although the surface shows some odd markings which have not been explained but which may correspond to a less localized bombardment. The erosion, however, is markedly less. Measurements taken on representative anodes indicate that at 200 hours the high inverse tube has lost 40 milligrams of molybdenum while the low inverse has lost only 20 milligrams.

Figure 2 (c) shows an anode taken from tube 1736 run at 5600 cycles, $\frac{1}{4}$ microsecond with an inverse of 3200 volts. Again the erosion is less severe than in the case of the high inverse tube but more severe than was observed in the JAN test. Some drilling has taken place completely through as evidenced by the markings on the grid in back of the anode. Figure 2 (d) shows the anode from tube 2875 which should be compared with Fig. 2 (a) since both tubes were run under the same nominal conditions except that tube 2875 lasted only 98 hours as compared to 200 hours for tube 2597. The reason is apparently to be found in the obviously much more local discharge of the 2875. It is apparent that a portion of the anode has been heated to very high temperatures and that the erosion in that portion is very severe. Since the general observation is that these tubes have failed because of lack of adequate grid dissipation to absorb the power from overheated anodes, this comparison tends to further substantiate the conclusion. The localized discharge has created a higher temperature, a higher local power dissipation and thus a shorter life.

These results are summarized in Fig. 4 where is plotted the number of tubes remaining as a function of life for each of the three tests discussed above. The 2800 cycle JAN life test is presented for

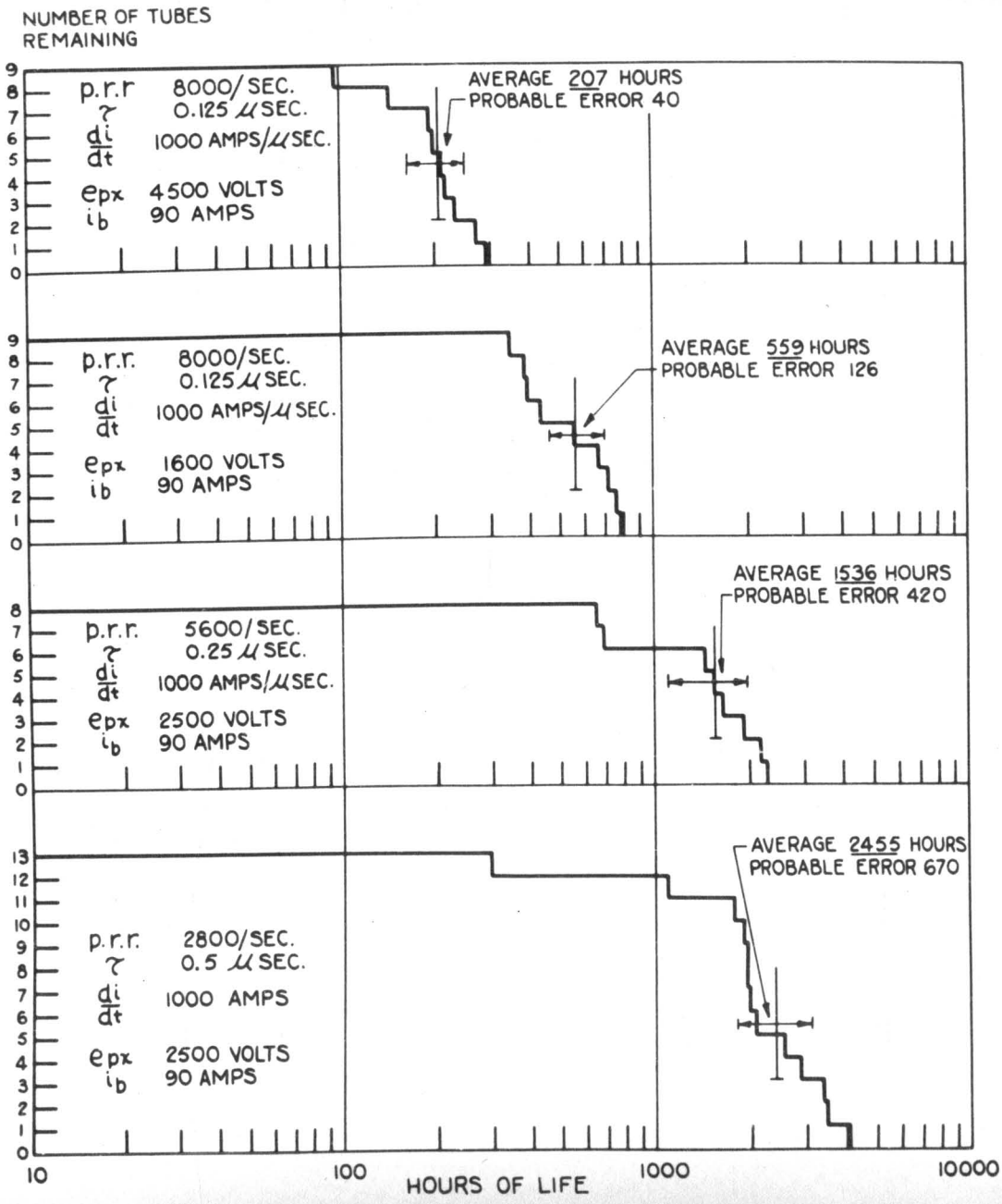

Fig. 4 Number of tubes remaining as a function of life.

comparison. There seems to be little doubt but that a distinctly separate life can be attributed to each test since the overlap of the distributions is not as large as the differences in the averages. This is particularly true of the third and fourth test running at high repetition rate with differing inverse voltages. Thus, it is safe to conclude that:

a) There is a qualitative distinction between the causes of life failures at high and low repetition rates but at the same average and peak power.

b) This distinction will be evidenced by failure from cathode depletion at low repetition rates or too much anode dissipation at high repetition rates.

c) At the high repetition rates where the latter cause of failure is dominant, inverse voltage plays a very important part in the determination of tube life.

Several investigations have been made on the mechanism of the effect of inverse voltage. The most striking phenomenon is, of course the erosion of the anode material which appears to be sputtered by positive ions coming through the grid holes. This sputtering must be accompanied by a substantial amount of local heat production. Evidence of this may be seen in Fig. 5 which is a photomicrograph of an erosion pit in the molybdenum anode of a 1754 which has seen service under very violent inverse conditions. This tube was run 75 hours under Operation 1 conditions (27.5 kv, 1.1 amperes) following which it was run for 20 hours at 1500 cycles 17 kv, 1.3 microseconds, 15-ohm load in a Western Electric magnetron ageing kit. Under these conditions it is very likely

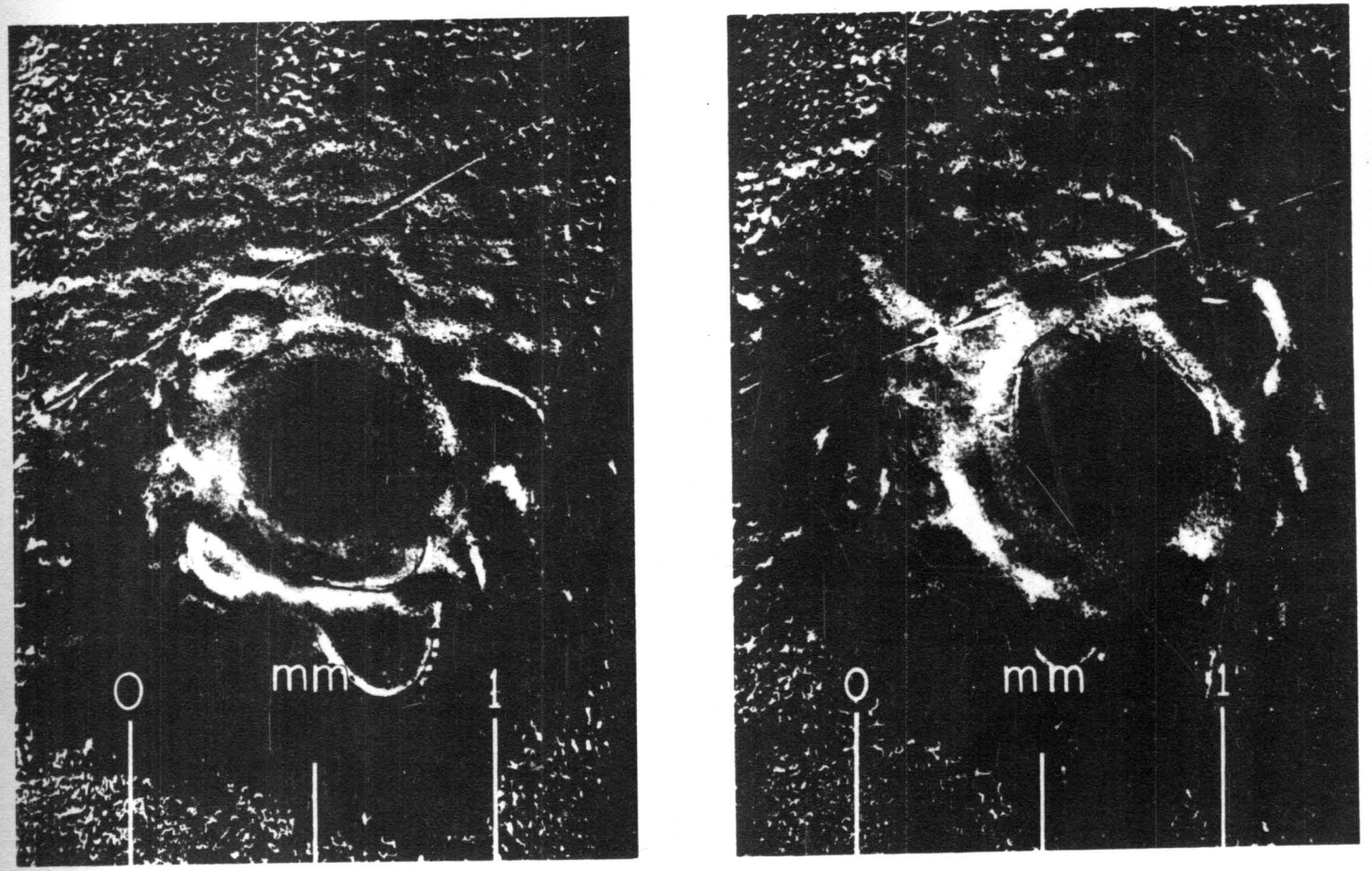

Fig. 5 Erosion pit in the molybdenum anode of a 1754.

that the inverse voltage was of the order of 17 kv. It is apparent that the bombarded surface has reached a temperature sufficient for molybdenum to melt locally as evidenced by the waves of frozen molten material around the hole. The hole itself has probably been produced partially by evaporation but mostly by the pressure of the beam of positive ions striking the surface. On the basis of current and voltage measurements made on the 4C35 one may estimate that the pressure exerted is of the order of an atmosphere.

Another interesting feature of Fig. 2 is the presence of the holes drilled in that portion of the grid which lies directly in back of the anode. Since the ions were accelerated to the anode from the grid holes in the first place, they could not arrive here with excess energy unless the voltage had changed appreciably during the time of transit. Thus we expect to find that the inverse voltage causing trouble must vary in a very rapid manner and exhibit a very sharp peak.

Figure 6 is a measurement of the inverse voltage and the positive ion current that flows to the anode at the same time. This voltage was measured with the circuit indicated "measurement circuit" in the same figure. Because of the effect of stray capacitance across the diode used to establish the zero of potential the true shape of the voltage must be deduced by measurements of the circuit parameters. This deduced voltage is labelled "actual" and, as expected, exhibits a very sharp peak at about 50 millimicroseconds after the end of the pulse. The positive ion current also shown reaches a peak of about 10 amperes for these particular conditions in about 25 millimicroseconds and is substantially zero at the end of 100 millimicroseconds. In spite of

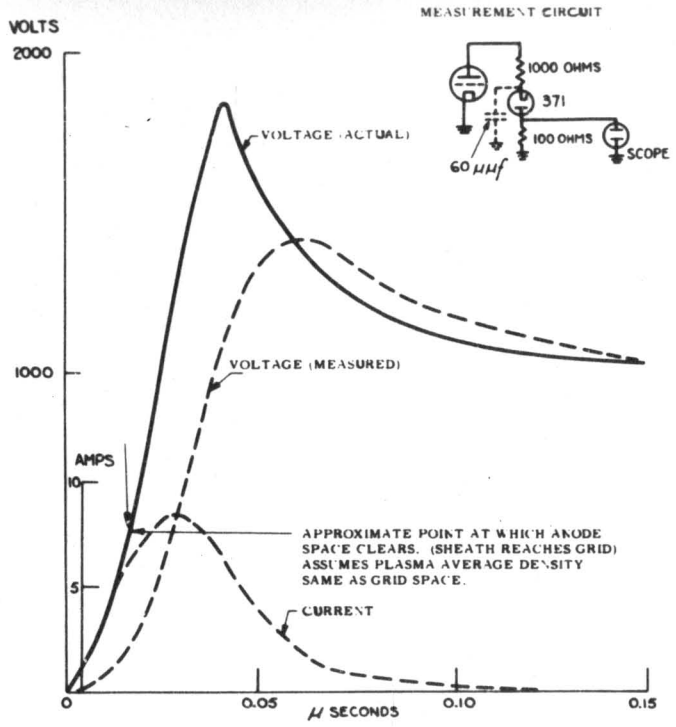

Fig. 6 Inverse voltage and current. Forward anode current 120 amperes.

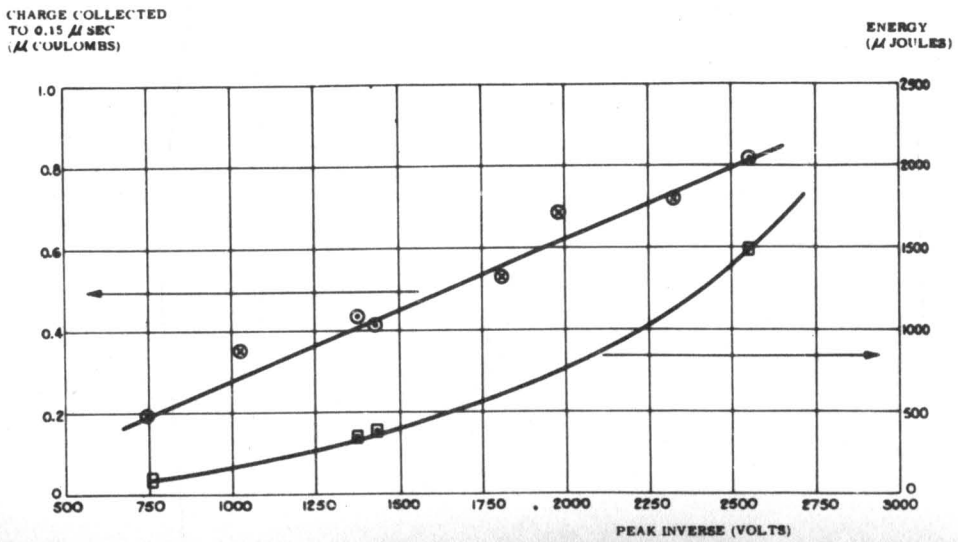

Fig. 7 Charge collected as a function of inverse voltage.

the fact that nearly a millijoule of energy has been expended at the anode, roughly 90% has appeared in only 50 millimicroseconds. It is with no little suprise that we discovered the effect of this remarkably short time burst of current. The source of the current is of course the positive ions in the plasma. The source of the voltage spike is evidently the energy stored in the stray inductance in the anode circuit. It is very likely that this voltage clears the ions from the space between anode and grid in something of the order of 20 millimicroseconds so that from this time on ions are flowing through the grid holes from the plasma contained in the cathode-grid space. This is the reason why holes are drilled opposite the grid holes.

The inverse voltage appearing in this short interval following the end of the current pulse can be varied by manipulation of the pulse-forming network while at the same time holding the peak forward current constant. The results of such a measurement are shown in Fig. 7 which shows the charge collected as a function of inverse voltage out to 150 millimicroseconds.

Since the positive charge in the plasma is proportional to the peak forward current (See Page 26 Fifth Quarterly Progress Report), the total positive charge collected by the anode should be substantially independent of inverse voltage in this measurement. As indicated by the results so far displayed, it varies nearly linearly with voltage, instead. Thus there must either be some mechanism of multiplication at work or the volume from which ions are collected must increase with the voltage. The appearance of Figs. 2 and 5 indicates that the anode surface may have been hot enough for thermionic emission

in these tests. If this is the case, then the calculation of the power dissipated is made difficult since the fraction of current carried by electrons leaving the anode cannot be measured directly.

On the assumption that thermionic emission is not taking place from the anode, the curve in Fig. 7 showing energy in microjoules as a function of inverse voltage has been calculated from the measurement of charge collected. This value will certainly represent the maximum.

At 2500 volts peak inverse, the energy per pulse was about 1500 microjoules at 120 amperes corresponding to 1000 microjoules at 90 amperes. At a repetition frequency of 10,000 cycles, this would mean a dissipation of 10 watts. Under similar conditions the "spike" energy at the start of the pulse has been estimated as about 500 microjoules (see Page 22 Third Quarterly Progress Report). Thus, the inverse dissipation may easily outweigh that of the "spike".

Fortunately, it appears likely that this source of dissipation may be controlled by proper attention to the constants of the pulse forming network. Consider first a single section network, as shown in Fig. 8.

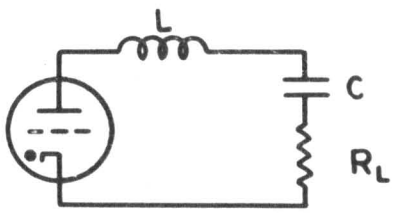

Fig. 8 Single section pulse forming network.

Assume that the tube becomes an open circuit at the instant the current falls to zero. At this moment, the condenser voltage is

$$V_c = - L \left. \frac{di}{dt} \right|_{i=0} \tag{A}$$

which will then appear across the tube. It is easy to show that this voltage for the case mentioned above is

$$V_c = - e_{p4} e^{- \frac{\alpha}{\beta} \pi} \equiv e_{px} \tag{B}$$

where

$$\alpha = R/2L$$
$$\beta = \sqrt{\omega^2 - \alpha^2}$$
$$\omega^2 = 1/LC$$

It is interesting that if we let

$$Z_o = 2\sqrt{\frac{L}{C}} \tag{C}$$

then

$$\ln \left| \frac{e_{p4}}{e_{px}} \right| = \frac{R\pi}{\sqrt{Z_o^2 - R^2}} \tag{D}$$

a quantity which does not depend explicitly on L.

If a current, i_i, may flow momentarily in the reverse direction in the tube as a result of the collection of positive ions or anode electron emission, or whatever, and the total charge involved is small compared to that stored in the condenser, then

$$e_{px} = -V_c + L\frac{di}{dt} \qquad (E)$$

where i_i = inverse current

or

$$e_{px} = -e_{py}\, e^{-\frac{\pi R}{\sqrt{Z_o^2 - R^2}}} + L\frac{di}{dt} \qquad (G)$$

The first term is the value calculated on the assumption of no inverse current. The second term will first be positive and then negative if the current behaves as shown in the data of Fig. 6. Thus the actual inverse voltage will at first be less than that calculated and then greater, and in fact will be expected to have an appearance corresponding to that in Fig. 6, where it will be noticed that the peak corresponds exactly to a maximum in the rate of decrease of current.

The variation of inverse current with time has not been determined, and so an explicit relation for the variation of inverse voltage during the time it is flowing has not been derived. However, From Fig. 6 the maximum rate of decrease of inverse current is about $\frac{20}{6 \times 10^{-2}} \approx 3 \times 10^2$ amps/microsecond. The inductance involved is about one microhenry so that the peak inverse is at least 300 volts higher than might have been calculated. It is very apparent that the

entire peak of 700 or 800 volts lying above the plateau at about 1000 volts can be accounted for in this manner.

In a very similar manner one may consider the behavior of a transmission line network originally charged to a voltage V_o, and discharging into a load consisting of inductance and resistance, as shown in Fig. 9.

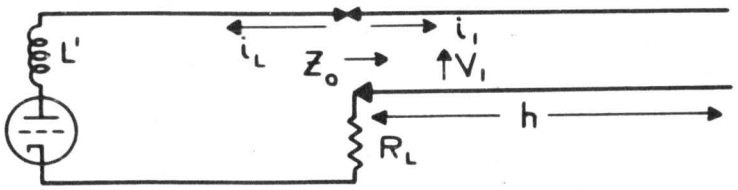

Fig. 9 Transmission line network.

At $t=0$, conduction commences.

Let:

V_1 = voltage wave on transmission line

i_1 = current wave on transmission line

h = length of line

Z_o = characteristic impedance

i_L = load current

L' = load inductance, total

R_L = load resistance

V_o = voltage to which transmission line is charged (e_{py})

Now

$$i_L = -i_1$$

$$V_1 = Z_o i_1$$

$$L' \frac{di_L}{dt} + R_L i_L = V_o + V_1 \qquad (H)$$

Thus at x = o

$$i_L = \frac{V_o}{R_L + Z_o}\left(1 - e^{-\alpha t}\right) \tag{I}$$

The current wave on the transmission line is

$$i_1 = -\frac{V_o}{R_L + Z_o}\left(1 - e^{-\alpha(t - x/c)}\right) \tag{J}$$

where c = velocity of propogation on the transmission line

$$\alpha = \frac{R_L + Z_o}{L}$$

When $t = h/c$, i_1 is reflected from the open end of the line ($x = h$), thereafter, until the reflected wave reaches the load, the total current is the sum of i_1 and its reflection i_2.

Since, at x = h

$$i_1 + i_2\big|_{x=h} = 0$$

$$i_2 = \frac{V_o}{R_L + Z_o}\left(1 - e^{-\alpha\left(t - \frac{h}{c} - \frac{h-x}{c}\right)}\right) \tag{K}$$

At $t = 2h/c$, i_2 reaches the load end and a reflection, i_3, occurs in order that Kirchoff's law be obeyed at the terminal.

$$-i_L = i_1 + i_2 + i_3\big|_{x=0}$$

Now

$$V_L = V_o + V_1 + V_2 + V_3\big|_{\substack{x=0 \\ t > \frac{2h}{c}}} \tag{L}$$

and

$$V_1 = Z_o i_1$$
$$V_2 = -Z_o i_2$$
$$V_3 = Z_o i_3$$

At x = o $$L' \frac{di_L}{dt} + i_L R_L = V_L$$

Thus $$L' \frac{di_L}{dt} + (R_L + Z_o) i_L = V_o - 2Z_o i_2 \Big|_{x=o}$$

$$= V_o \left(\frac{R_L - Z_o}{R_L + Z_o} \right) \left(1 + \frac{2Z_o}{R_L - Z_o} e^{-\alpha \left(t - \frac{2h}{C} \right)} \right) \quad (M)$$

When

$$t = \frac{2h}{C} \text{ (assumed } >> 1/\alpha), \quad i_L = \frac{V_o}{R_L + Z_o}$$

Accordingly the solution of (M) is:

$$i_L = V_o \frac{R_L - Z_o}{(R_L + Z_o)^2} \left(1 + \frac{2Z_o}{R_L - Z_o} \alpha t' e^{-\alpha t'} + \frac{2Z_o}{R_L - Z_o} e^{-\alpha t'} \right) \quad (N)$$

where

$$t' = t - \frac{2h}{C}$$

(t' is measured from the instant the reflected current, i_2, reaches the load)

At the instant of zero current, the voltage on the line is $L' \, di_2/dt$ and, if i_L remains zero, it is this voltage which is applied as inverse to the tube. This instant, t'_o is determined by setting equation (N) equal to zero.

$$\frac{2Z_o}{Z_o - R_L} e^{-\alpha t'_o} \left(1 + \alpha t'_o \right) = 1 \quad (P)$$

This transcendental equation may be solved graphically for its roots, as show in Fig. 10. The quantity of $\alpha t'_o = \frac{R_L + Z_o}{L'} t'_o$ varies from a least value of about 1.7 upwards as $\frac{R_L}{Z_o}$ varies from zero to unity. The variation is very slow until $\frac{R_L}{Z_o}$ is very close to unity. For example, if

$$\frac{R_L}{Z_o} = 0.96, \quad \alpha t'_o = 5.8$$

After the tube has ceased conduction, the voltage across it is

$$e_{px} = V_o + V_1 + V_2 + V_3$$

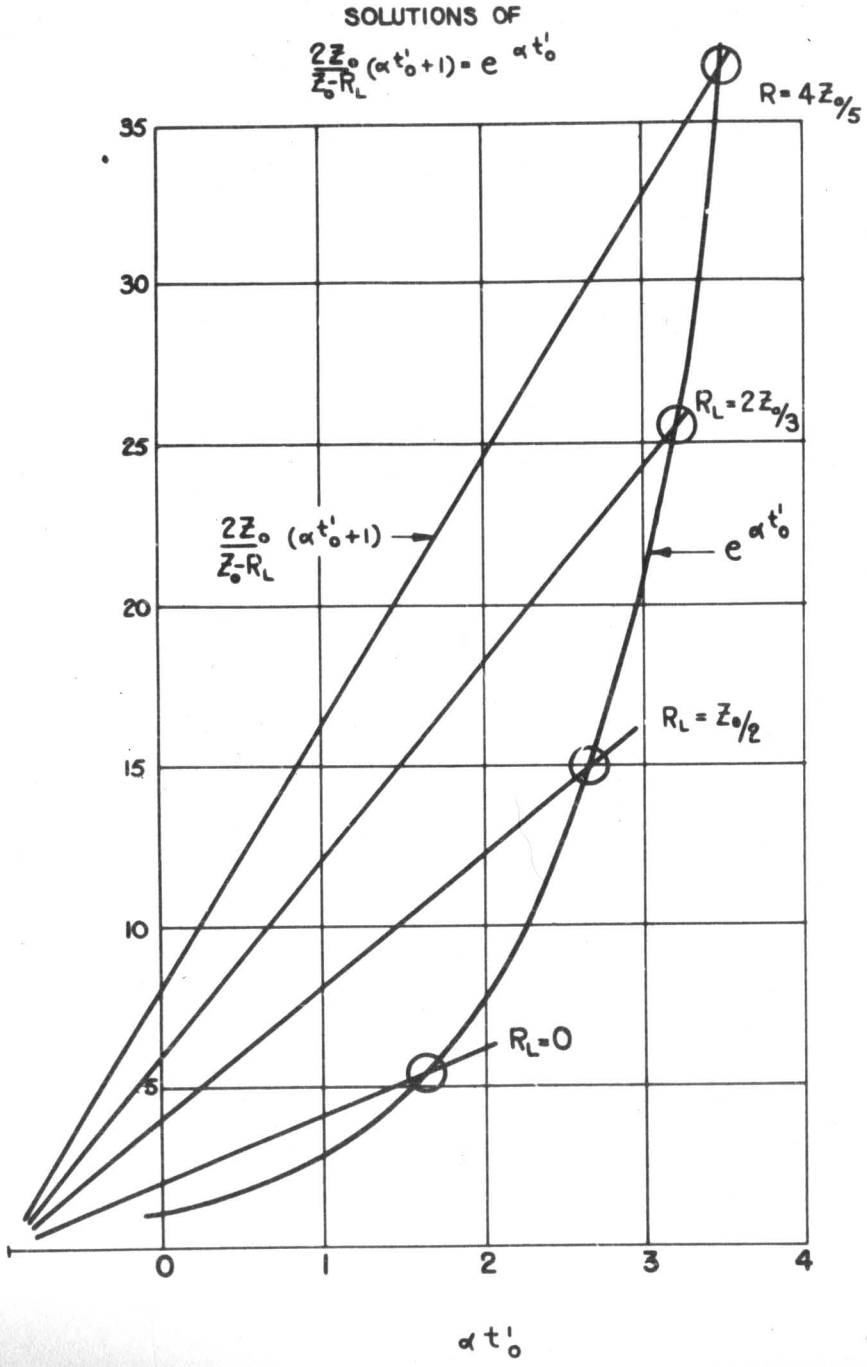
SOLUTIONS OF
$\frac{2Z_o}{Z_o-R_L}(\alpha t'_o+1) = e^{\alpha t'_o}$
$R = 4Z_o/5$
$R_L = 2Z_o/3$
$R_L = Z_o/2$
$R_L = 0$
$\frac{2Z_o}{Z_o-R_L}(\alpha t'_o+1)$
$e^{\alpha t'_o}$
35
30
25
20
15
10
5
0
1
2
3
4
$\alpha t'_o$

Fig. 10

until the current wave i_3 has traveled to the end of the transmission line, been reflected and arrives again at the load end. During this interval

$$i_1 + i_2 + i_3 = 0 \qquad (Q)$$

and

$$e_{px} = V_o \frac{R_L - Z_o}{R_L + Z_o} \left(1 + \frac{2Z_o}{R_L - Z_o} e^{-\alpha t'}\right)$$

Thus in the absence of any inverse conduction, (which will be discussed presently) the inverse voltage appears instantaneously at t'_o and has the value

$$V_o \frac{R_L - Z_o}{R_L + Z_o} \left(1 + \frac{2Z_o}{R_L - Z_o} e^{-\alpha t'_o}\right)$$

which is somewhat less than the ideal value

$$V_o \frac{R_L - Z_o}{R_L + Z_o}$$

to which it rises in an exponential manner. The factor $1 + \frac{2Z_o}{R_L - Z_o} e^{-\alpha t'_o}$ is shown in Fig. 11 as a function of R_L/Z_o.

Between the arrival of i_2 at the load end of the transmission line and the instant that the load current becomes zero (t'_o), i_3, the reflection demanded by Equation (L), goes through a minimum and is positive at $t = t'_o$.

$$i_3\Big|_{x=o} = -i_L + \frac{V_o}{R_L + Z_o} e^{-\alpha t'}$$

if $o < t' < t'_o$ $\quad i_3 = -\frac{V_o (R_L - Z_o)}{(R_L + Z_o)^2} \left\{1 - e^{-\alpha(t' - \frac{x}{c})} + \frac{2Z_o}{R_L - Z_o} \alpha (t' - \frac{x}{c}) e^{-\alpha(t' - \frac{x}{c})}\right\}$

if $t'_o < t'$ $\quad i_3 = \frac{V_o}{R_L + Z_o} e^{-\alpha(t' - \frac{x}{c})} \qquad (R)$

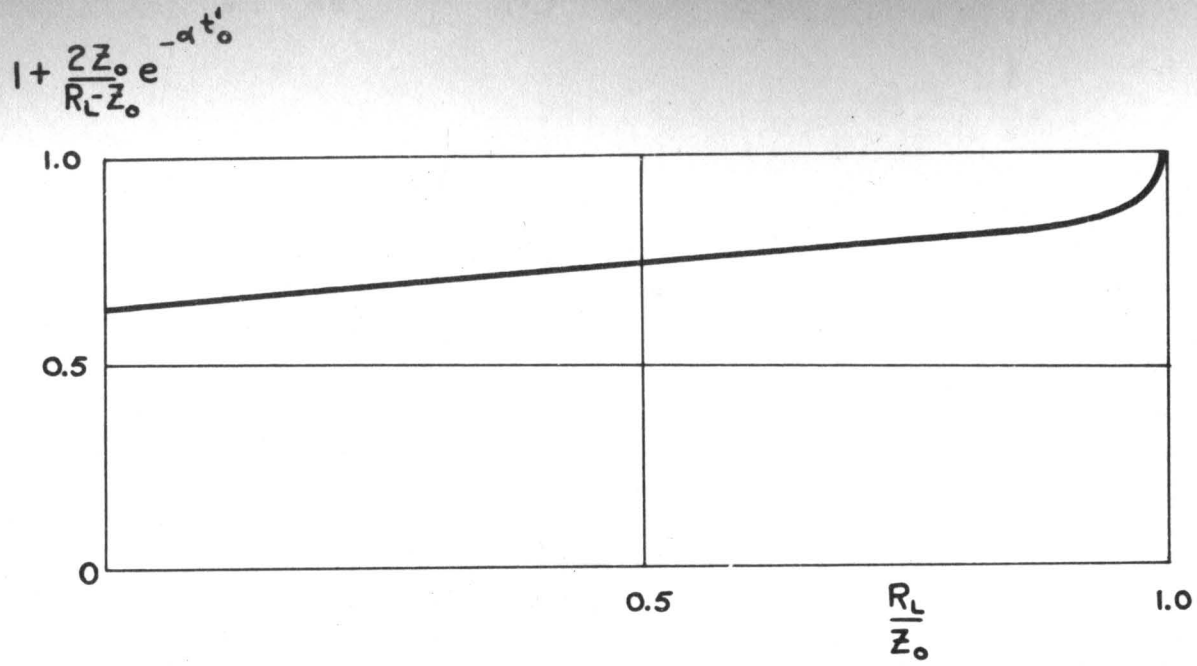

Fig. 11 $1 + \frac{2Z_o}{R_L - Z_o} e^{-\alpha t'_o}$ as a function of R_L / Z_o.

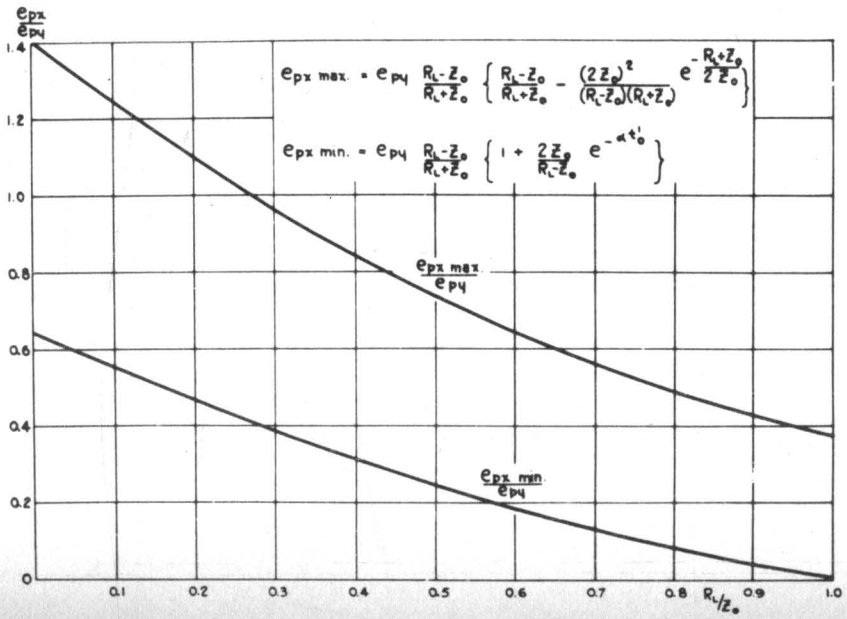

Fig. 12 Limits of oscillation as functions of R_L / Z_o.

This current will be reflected at the open circuit at the "far end" of the line and return to the load end in time $\frac{2h}{c}$. This end is now also assumed to be an open circuit, so that another reflection takes place, and so on. The voltage developed at the open circuit terminals, is of course

$$V = 2Z_o i_3 \Big|_{x=0}$$

Accordingly, the inverse voltage appearing at x = 0 will oscillate between

$$V_o \frac{R_L - Z_o}{R_L + Z_o} \left(1 + \frac{2Z_o}{R_L - Z_o} e^{-\alpha t'_o}\right)$$

and

$$V_o \left(\frac{R_L - Z_o}{R_L + Z_o}\right) \left\{\frac{R_L - Z_o}{R_L + Z_o} - \frac{(2Z_o)^2}{(R_L - Z_o)(R_L + Z_o)} e^{-\frac{R_L + Z_o}{2Z_o}}\right\}$$

That is, the inverse voltage will have a series of bumps on it caused by the reflection i_3 which will wash back and forth on the open-circuited line. This voltage will depend on $\frac{R_L}{Z_o}$, and varies from $-1.45V_o$ at $R_L = 0$ to a limit of $-0.37V_o$ as R_L approaches Z_o.

These two limits of oscillation are plotted as functions of $\frac{R_L}{Z_o}$ in Fig. 12. It is interesting that $e_{px\ (max)}$ is still an appreciable fraction of e_{py} even at $R_L = Z_o$. This comes about, of course, because of the voltage generated across the inductance during the falling part of the pulse. The inverse voltage as a function of time will appear as shown in Fig. 13.

The presence of current flowing in the reverse direction immediately following the end of the current pulse modifies this picture importantly in only two respects. First, the inverse voltage immediately after the end of the current pulse will now exhibit a sharp

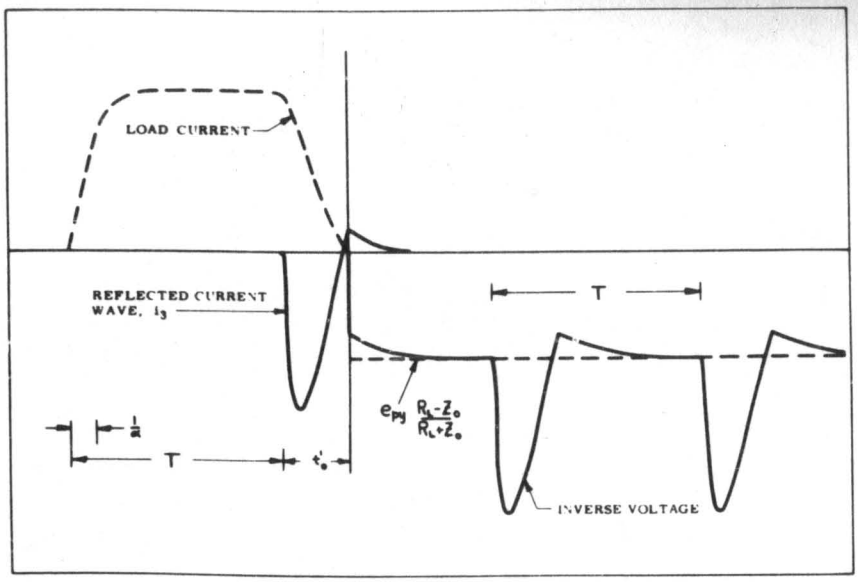

Fig. 13 Inverse voltage, load current and reflected current as a function of time. (Without inverse conduction.)

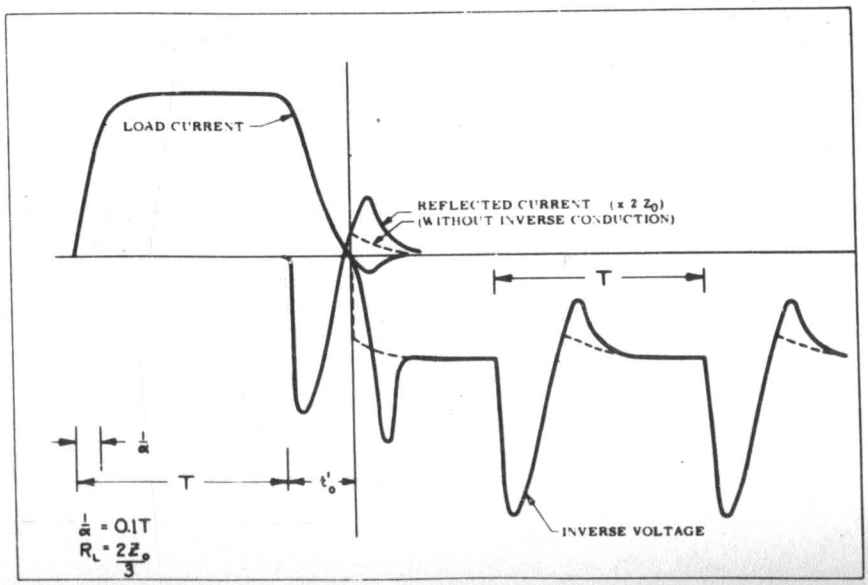

Fig. 14 Inverse voltage, load current and reflected current (including inverse conduction) as a function of time.

spike, as demonstrated experimentally in Fig. 6. Second, the minimum value of e_{px} will be substantially less than it otherwise would be. These features are exhibited in Figs. 14 and 15 and may be deduced as discussed below.

Suppose that the inverse current through the tube is a function of time, -f (t_1), following the cessation of forward current, as indicated by the data of Fig. 6. Time, t_1, is measured from t'_o, the instant of zero current. Then

$$i_L = -f(t_1) \qquad t_1 = t' - t'_o$$

The tube voltage is

$$e_{px} = -L' \frac{di_L}{dt} - R_L i_L + V_{Line} \tag{S}$$

where

$$V_{Line} = V_o + Z_o (i_1 - i_2 + i_3)$$
$$-i_L = i_1 + i_2 + i_3$$

Thus, as before

$$V_{Line} = V_o - 2Z_o i_2 - Z_o i_L \tag{T}$$

and

$$e_{px} = L' \frac{df}{dt} + (R_L + Z_o) f + V_o \left(\frac{R_L - Z_o}{R_L + Z_o}\right) \left\{ 1 + \frac{2Z_o}{R_L - Z_o} e^{-\alpha(t'_o + t_1)} \right\} \tag{U}$$

The final term of Equation (U) is of course the inverse voltage deduced when there is no inverse current flowing.

The relations of Equation (U) are demonstrated graphically in Fig. 15 where several voltages are drawn separately, and the sum. The resulting peak depends on the relative magnitude of L' and $R_L + Z_o$. The function f (t_1) is shown multiplied by $R_L + Z_o$. The sum of $L' \frac{df}{dt_1}$ and $(R_L + Z_o) f$ is shown as the dashed curve. The inverse with zero conduction is also displayed. At $t_1 = 0$ where $i_L = 0$ the voltage drop across L' is just equal and opposite to the inverse calculated

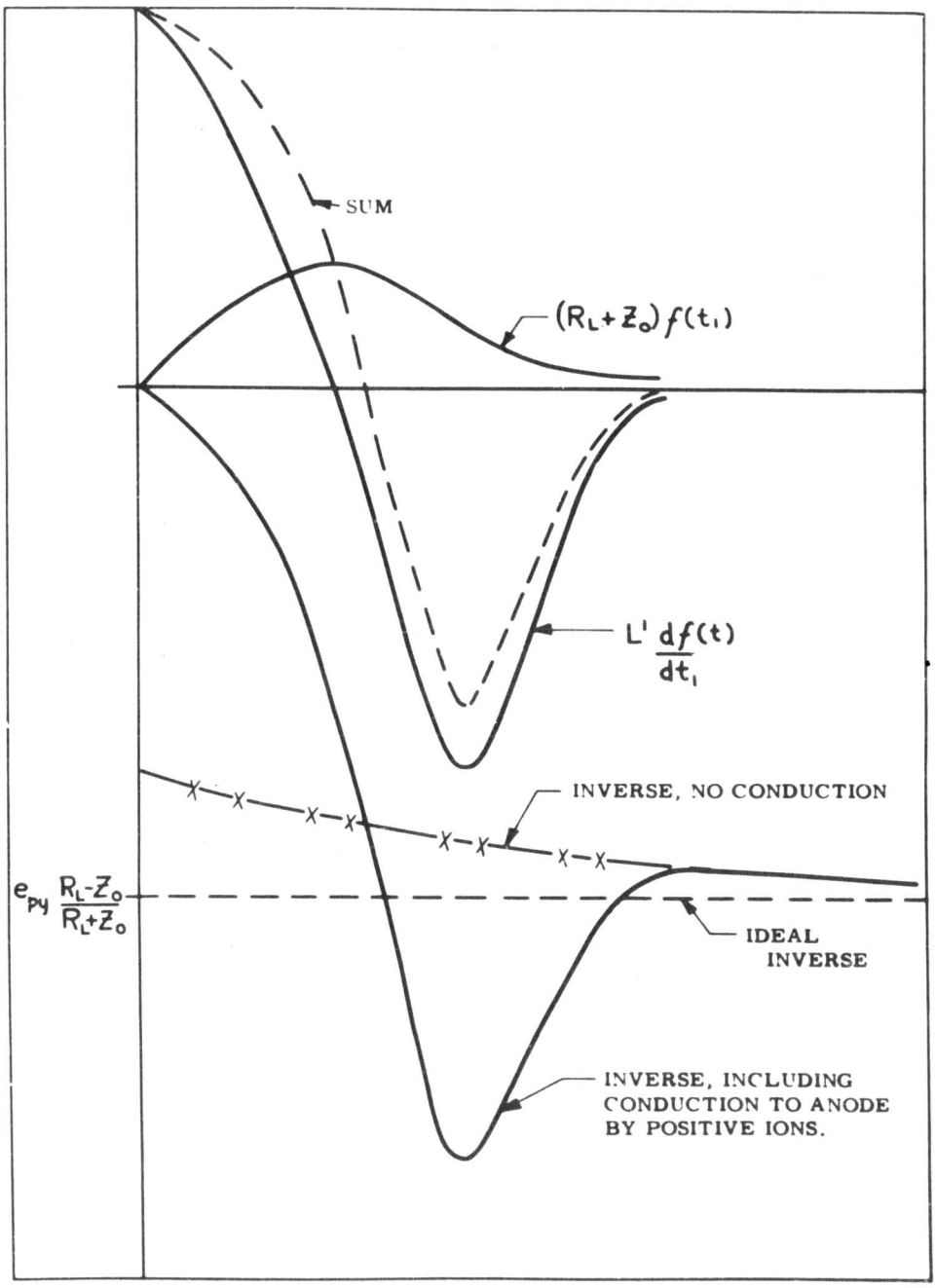

Fig. 15 Details of the formation of the "spike" inverse voltage from inverse current.

for no conduction, i.e., $e_{px} = 0$ at $t_1 = 0$. Since experimentally the function $f(t_1)$ taken from Fig. 6 has approximately the same magnitude of slope on either side of its maximum, the maximum inverse is shown to be about twice the no-conduction inverse at $t_1 = 0$. (Of course this particular detail need not be general and will depend on the particular way current flows during the application of inverse voltage.) The duration of $f(t_1)$ is shown to be approximately the same as $\frac{1}{\alpha}$ as was the case in Fig. 6. Again this detail is coincidental.

As a result of the flow of inverse current, the reflection on the line, i_3, is changed after t'_0 from Equation (R).

From Equation (S)

$$i_3\Big|_{x=0} = f(t_1) - i_1 - i_2$$

$$\text{if } 0<t_1 \quad i_3\Big|_{x=0} = f(t_1) + \frac{V_o}{R_L+Z_o}\, e^{-\alpha(t'_o+t_1)} \tag{V}$$

$$i_3 = f\left(t_1-\tfrac{x}{c}\right) + \frac{V_o}{R_L+Z_o}\, e^{-\alpha t'_o}\, e^{-\alpha\left(t_1-\frac{x}{c}\right)}$$

Before this instant ($t_1 = 0$) i_3 is the same as given in Equation (R).

$$-t'_o< t_1<0 \quad i_3 = -V_o\frac{R_L-Z_o}{(R_L+Z_o)^2}\left\{1-e^{-\alpha\left(t'_o+t_1-\frac{x}{c}\right)} + \frac{2Z_o}{R_L-Z_o}\,\alpha(t'_o+t_1)\,e^{-\alpha\left(t'_o+t_1-\frac{x}{c}\right)}\right\} \tag{W}$$

The terminal voltage resulting from the successive reflections of this current are found in a manner similar to that used in deriving Equation (Q).

Thus, at the first arrival after the end of the pulse

$$e_{px}\Big|_{t_1>\frac{2h}{c}} = V_o\frac{R_L-Z_o}{R_L+Z_o}\left\{1+\frac{2Z_o}{R_L-Z_o}\,e^{-\alpha\left(t'_o+t_1-\frac{2h}{c}\right)} + 2Z_o\, i\left(t_1-\tfrac{2h}{c}\right)\right\} \tag{X}$$

Comparing Equation (X) with Equation (Q) it is apparent that the effect of the inverse current is to make the inverse oscillations of greater peak to peak amplitude than they would be if no inverse current flowed. The effect of inverse current is to generate an initial spike in the inverse voltage and to decrease the subsequent minima, as shown in Fig. 14 which represents the following conditions:

$$\text{Max Inverse Current} = 0.1\,\frac{V_o}{R_L+Z_o}$$

$\frac{1}{\alpha} = 0.1\,T$ (corresponds to about 1000 amps/microsecond JAN specification if peak current 90 amperes.)

T = "Two way transit time" of pulse network; i.e., $\frac{2h}{c}$, h = line length.

$$R_L = \frac{2Z_o}{3}$$

$$1+\frac{2Z_o}{R_L-Z_o}\,e^{-\alpha t'_o} \approx 0.8 \qquad \text{(See Fig. 11)}$$

$$\alpha t'_o \approx 3.2$$

$$i_3\Big|_{t'_o} \approx \frac{1}{25}\,\frac{V_o}{R_L+Z_o} \qquad \text{(See Fig. 10 and Equation (R))}$$

In this figure the current becomes zero at $t_1 = 0$. The load current flows in the forward direction for a time $T + t'_0$. The inverse current has been chosen in relation to forward current to be similar to that actually observed in Fig. 6. At the end of the current pulse the reflected current on the transmission line is shown magnified by a factor of three, which is the multiplier producing the correct terminal voltage (to this scale) resulting from its reflection from an open circuit. Dashed lines show the equivalent voltage when there is no conduction in the inverse direction.

It is interesting that the spike of voltage occuring immediately after the end of the current pulse may or may not exceed

the subsequent peaks depending on the coincidental relation between $L' \frac{df}{dt}$ and $(R_L + Z_o) f$ but that it never appears again.

That these conclusions do not require drastic modification to apply to a Type E network, which approximates a uniform transmission line, is evident from Fig. 16. Here are shown measurements of inverse voltage from a four section network, which display all of the qualitative features of the theoretical solution shown in Fig. 14. The agreement is surprisingly good.

It is apparent from reference to this figure that the principal effect of the discrete sections is to attenuate the details of the inverse oscillations after one or two reflections. Of course the high frequencies corresponding to the sharp peaks of Fig. 15 will not be propagated on such a network, so that the oscillations will be ultimately characterized by their fundamental component. In this respect the network can be represented by a uniform transmission line with an ideal low-pass filter inserted at its center.

It is apparent that the voltage spike appearing at the end of the current pulse is the most important part of the inverse voltage. Referring back to Fig. 15 it is evident that this spike is largely determined by the manner in which the inverse current decays, for a given inductance and resistance in the circuit. It is not possible to calculate the manner in which this will take place. The primary source of the inverse current is the positive ions left in the decaying plasma. The current would not, however, appear if no inverse voltage were applied to the tube. Thus the ideal inverse voltage (impedance mismatch) and the total positive ion charge in the tube, together determine the current

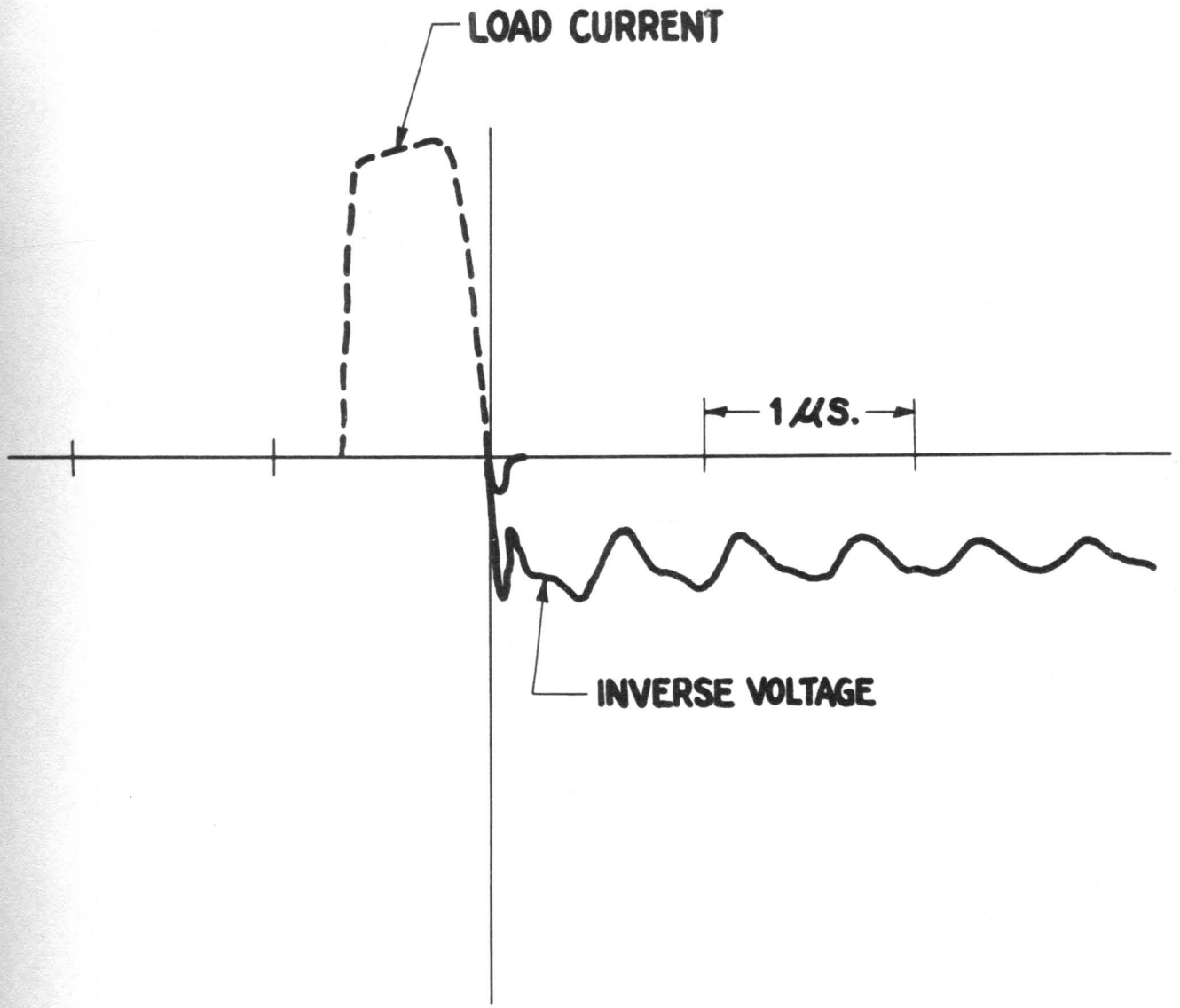

Fig. 16 Measurements of inverse voltage from a four-section network

during the inverse interval.

As a practical matter there is little that can be done about the positive ion charge. It is demonstrated in the Fifth Quarterly Progress Report (Page 26) that the separated positive charge is proportional to anode current. Thus the problem of dissipation during inverse conduction will be reduced with decreasing anode current. That is, for a given impedance mismatch, a high impedance circuit will lessen its effects. If the mismatch or ideal inverse voltage can be made very small then the power dissipated during the inverse will be reduced accordingly. In most applications the only useful purpose inverse voltage serves is to prevent the reapplied voltage from becoming sufficiently positive to re-ignite the tube until after the recovery interval. The necessity for it therefore diminishes as the frequency of operation is reduced. The maxima in the inverse voltage will have little effect on the tube dissipation, occuring as they do during a period when no current is flowing. The minima which are caused directly by the flow of inverse current in the characteristic impedance of the transmission line (See Fig. 14) can produce conduction if the impedance mismatch is small enough so that they drive the anode positive. In this case the apparent recovery time can be considerable prolonged.

While detailed measurements and analysis of the anode dissipation occuring during tube breakdown will not be undertaken until a later report, it is already apparent that the same inductance which slows down the rate of rise of current can be responsible for some features of the inverse voltage. As shown on Page 23 the ideal or mis-

match inverse voltage appearing across the tube at the end of the current pulse is $L' di/dt$. Thus the measures which tend to reduce dissipation during breakdown may be increasing it correspondingly at the end of the pulse if due care is not exercised.

1907 MODULATOR DESIGN AND CONSTRUCTION

A completed modulator unit has been constructed in accordance with the considerations for design of the critical modulator components as described in the Fifth Quarterly Report. Circuit components and general modulator layout are shown in Figs.17 and 18.

The oil cooled load, which is completely shielded can be seen as the cylinder in front of the pulse forming network (in the upper right hand corner of each figure directly behind the front panel). Cooling takes place in the heat exchanger shown on the top of the modulator. This consists of a standard finned tube held in a square frame with a fan to blow air through the structure. The oil, which is Dow-Corning Silicone fluid No. 200, is pumped through the load and then through the heat exchanger by a standard gear pump (Brown and Sharpe) (shown in the lower left hand corner of the modulator)driven by a 3/4 hp motor. Measurement of oil flow was not undertaken. A temperature of about 100° C is maintained at a power level of 6.5 kw average dissipation.

The internal arrangement of resistors is shown in Fig. 19 . The load for Operation 2 consists of six parallel resistors each of which is a 200-ohm, 160-watt Ohmite resistor (Stock #2407), making a 33-ohm unit. The other consists of three parallel 200-ohm, 100-watt Ohmite resistors (Stock #2207), making a total of 66 ohms. These two

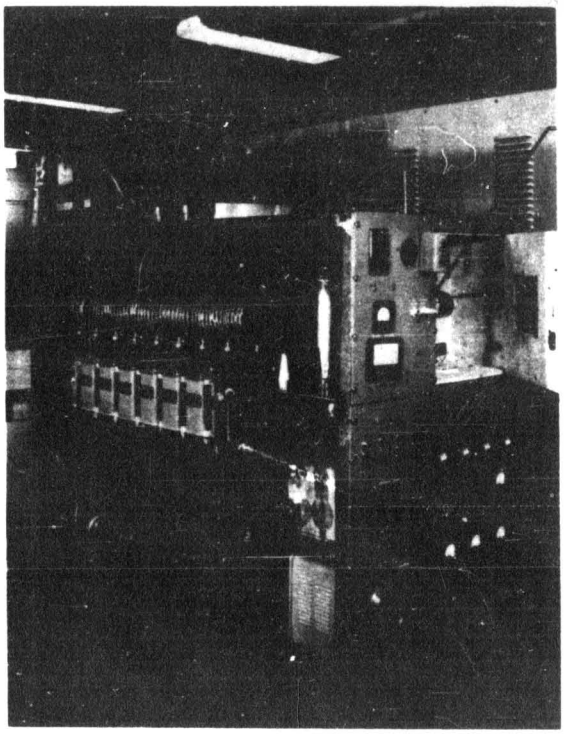

Current viewing connections

Fig. 17 General 1907 modulator layout.

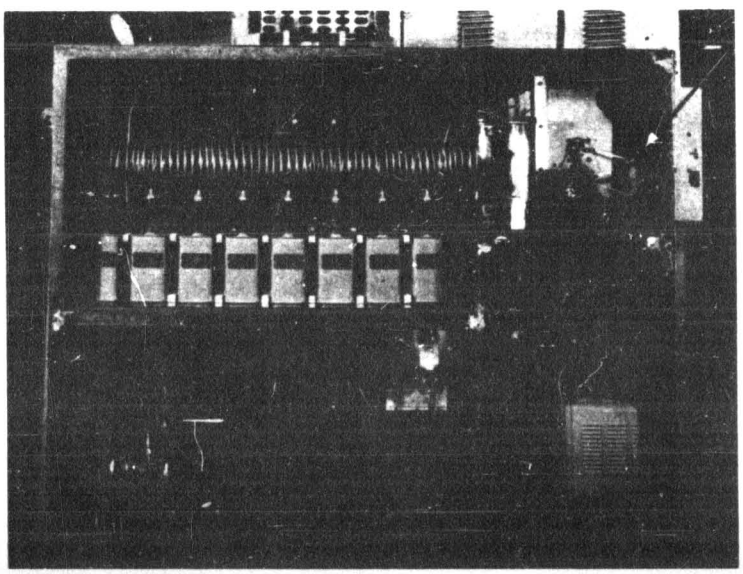

Current viewing resistor

Fig. 18 General 1907 modulator layout.

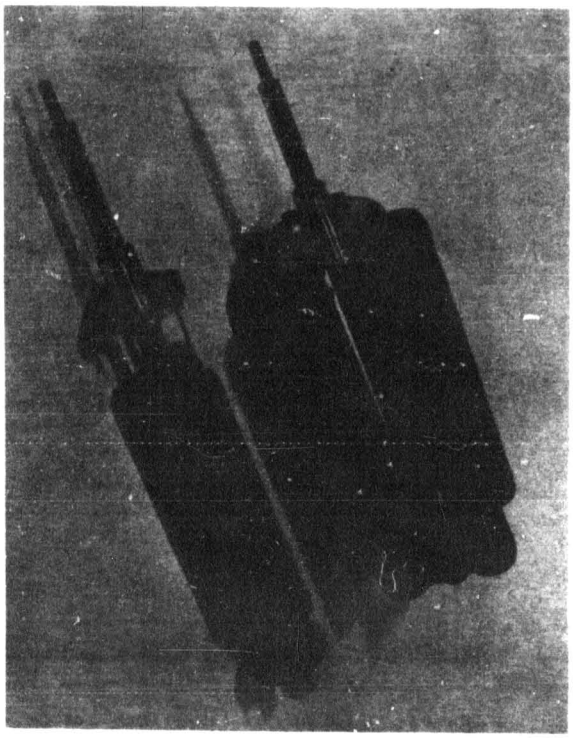

Fig. 19 Internal arrangement of load resistors.

units are connected in parallel for Operation 1 conditions where a load of 22 ohms is required. Fig. 20 shows the assembled load. The resistor assemblies fit concentrically into their respective can by screwing into a boss soldered into the base. The seal at the top is made with O-rings in the standard manner.

These loads have two distinct advantages. The first is that circuit inductance can be kept to a minimum, not only because of their compactness but because of the effect of paralleling several units.

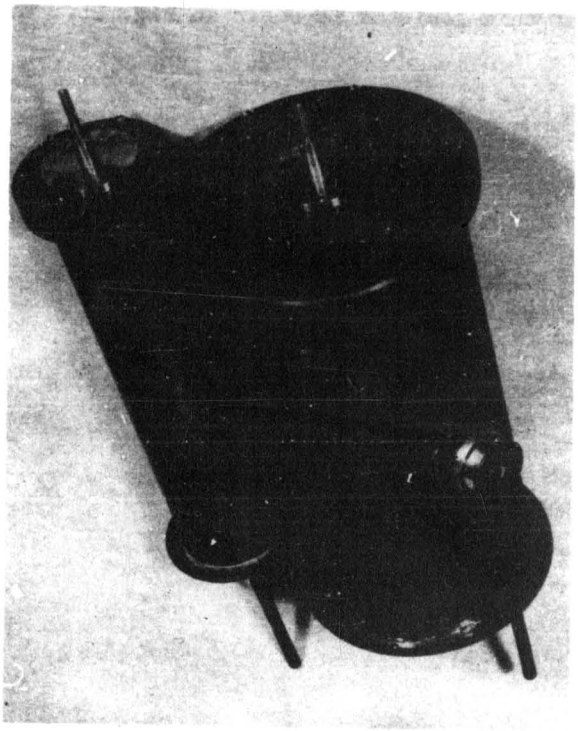

Fig. 20 Photograph of the assembled load resistors.

The second is that the heat dissipation from the unit takes place at a well defined location free from high voltage so that it may be easily vented. The small object seen in the side of the can in Fig. 20 is a thermostatically controlled switch which monitors the oil temperature. Should this rise above safe limits, the switch will activate an interlock to turn off the equipment.

The current viewing resistor is mounted on the back of the front panel as indicated in Fig. 18. The UHF connectors indicated in Fig. 17 allow direct access to the terminals of the resistor. A

photograph of this resistor is shown in Fig. 21. The vertical fins

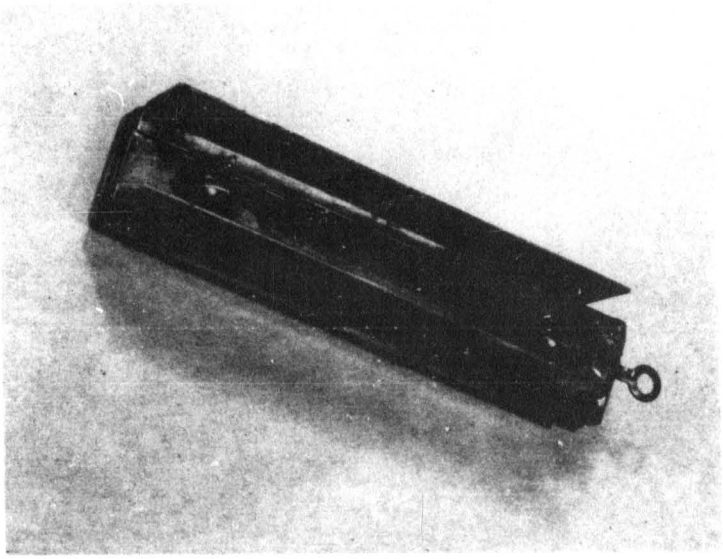

Fig. 21 Photograph of the current viewing resistor.

are provided for extra cooling since the resistor measures approximately 0.25 ohms and dissipates about 65 watts. Separate cooling is provided by a small blower mounted directly above it. An extremely low inductance has been achieved by constructing the resistor of a folded sheet of nichrome 0.002" thick by 1" wide and 5" long. This sheet is folded around a Teflon spacing sheet only 0.001" thick. The assembly is securely clamped by two 1/4" thick brass plates to insure minimum spacing between the nichrome sheets. The estimated inductance (obtained by calculation) is 0.25×10^{-3} microhenry. This construction is shown schematically in Fig. 22.

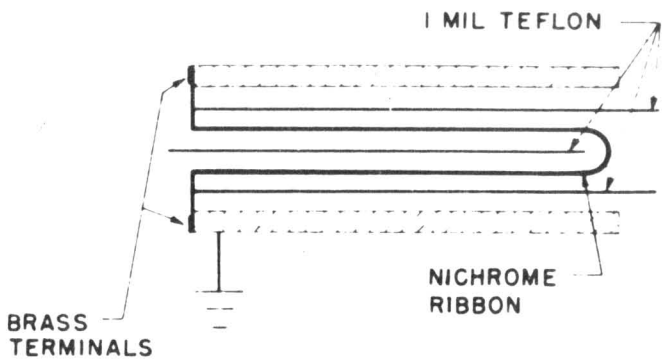

Fig. 22 Schematic diagram of current viewing resistor.

Current measurements in thyratron work are made difficult if the extremely high pulse currents circulate through any portion of the chassis. In this construction the point at which the resistor is bolted to the chassis is the ground return point for both the load and the current viewing cable. This prevents complication in the measurement from these currents. In this location the current viewing resistor is located as close as possible to the cathode pin of the tube socket. This has the additional advantage that the grid spike caused by cathode lead inductance is minimized. An oscillograph of this grid spike is shown in Fig. 23. In this figure the calibrating voltage marker is 100V. Thus the grid spike obtained under Operation 1 conditions is approximately 1,000V in amplitude.

A smooth rise and non-oscillatory current pulse was obtained by applying the principles developed during the construction of the 4C35 modulators discussed in the Second Quarterly Progress Report. As first constructed the rise of current was shown as in Fig. 24. The oscillations were found to be caused by the capacity of the filament

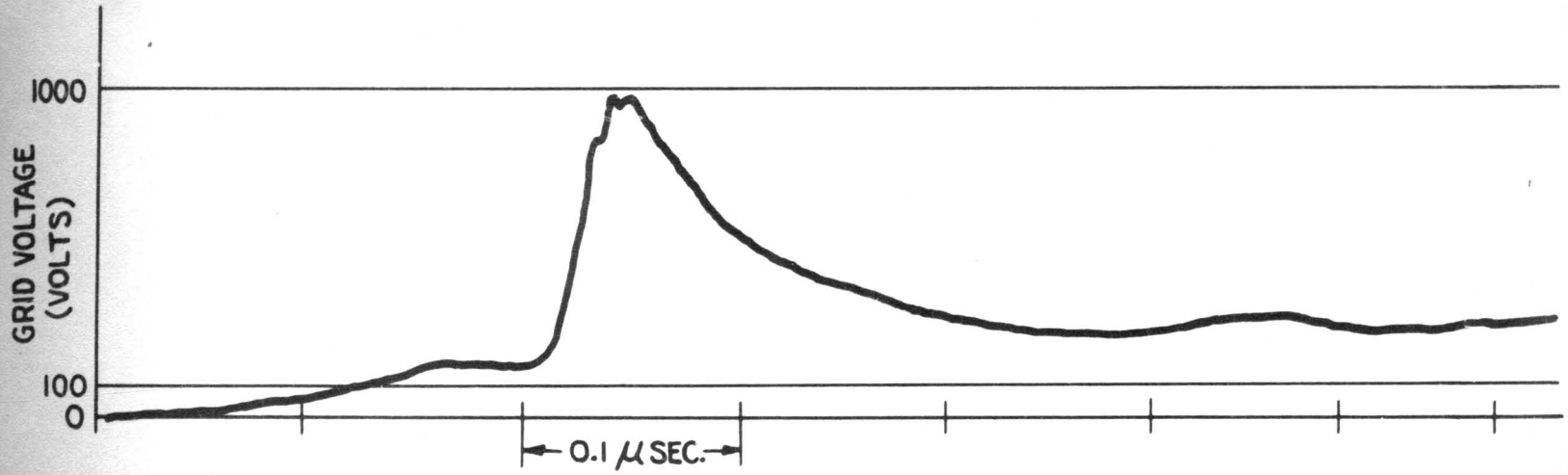

Fig. 23 Oscillograph tracing of the grid spike caused by cathode lead inductance.

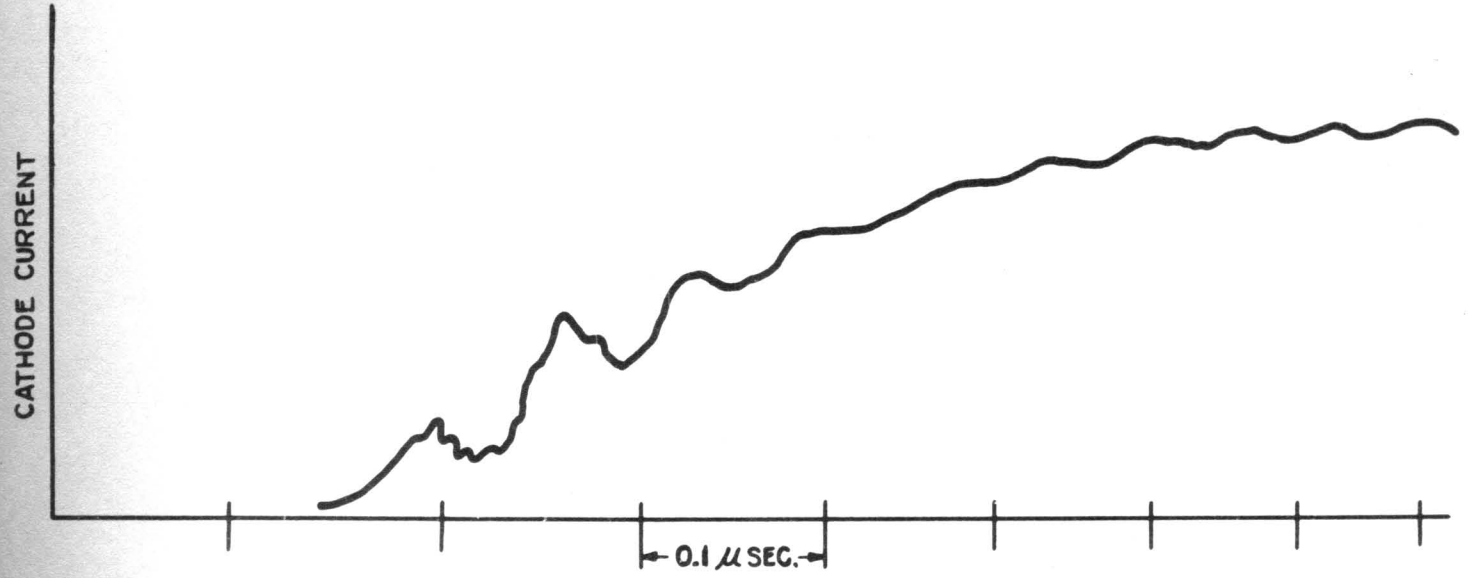

Fig. 24 Rise of current obtained with modulator as first constructed.

transformer for the charging diode. This capacitance was isolated with two 100-ohm, 10-watt wire-wound resistors in series. The current pulse so obtained is displayed in Fig. 25 . In making these adjustments, it is easy to be fooled if an improper reservoir setting for the tube is used. At low pressures the rate of fall of anode potential can be so slow that oscillations will not be excited. For example, Fig. 26 shows the rate of rise of current obtained by operating the tube at a reduced reservoir voltage (low enough to cause red anodes) but using the circuit unchanged from the conditions portrayed in Fig. 24 . The criterion for a proper test set up is that the rise of current be free from oscillations at any reservoir setting. In this connection it was found that the rate of rise of current was quite dependent on reservoir settings and degree of tube warm up. A variation from 2600 to 3200 amps/microsecond was observed over the normal range of operating conditions for a 1907 under Operation 1 testing (an 8-section, two-microsecond network was used). This complication was arbitrarily resolved by adding series inductance to the anode circuit until the rate of rise was reduced to 2500 amps/microsecond at the maximum reservoir voltage.

To date a single life test unit has been constructed and placed in operation so that a JAN life test has been in progress for some time. The construction of four additional life test units will be undertaken as soon as feasible.

THYRATRON DESIGN PROGRAMS

Parts and materials are being procured for a ceramic and metal envelope thyratron. Initial objectives of this program will be to establish

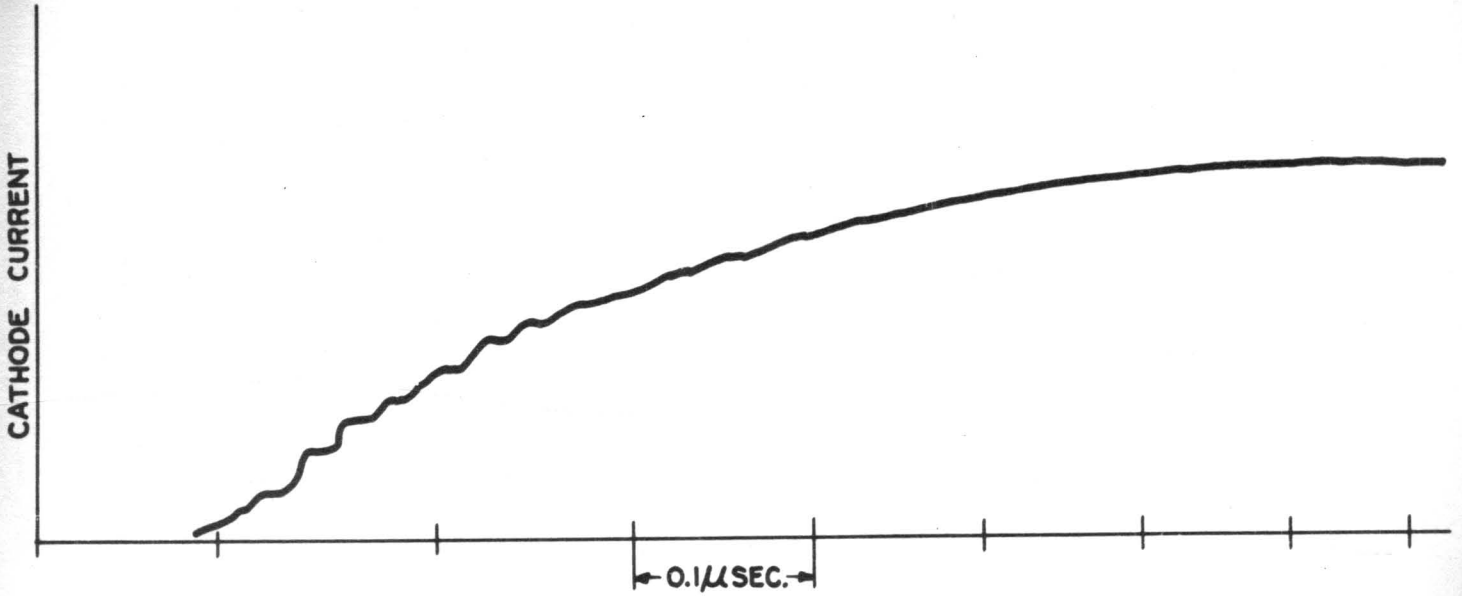

Fig. 25 Current pulse obtained with the filament transformer-charging diode capacitance isolated.

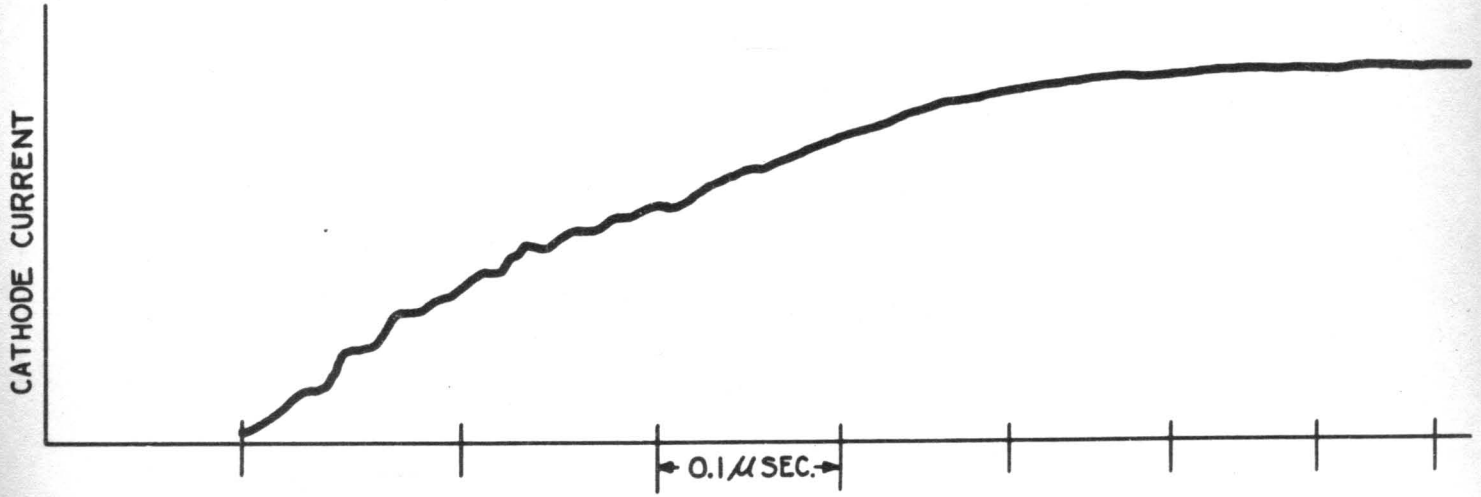

Fig. 26 Rate of rise of current when operating the tube at a reduced reservoir voltage.

the feasability of using certain envelope materials and also to develop assembly processes. Studies of grid and cathode characteristics will also be made on the initial assemblies.

A lead indium AI-200 to 326 stainless steel seal using the hydride process has been perfected here in relation to another application but the processes may be directly applied to the case of the thyratron configuration.

Figure 27 shows the basic design for a tube assembly using a low temperature solder. It will be noticed that vapor traps are applied at each seal to prevent high vapor pressure constituents of the ductile solder from entering the tube interior. The first tubes will be made with 4C35 cathode assemblies to simplify procurement of parts.

A ceramic-metal assembly has also been designed for assembly in a similar manner except that silver solders will be used for the final brazing. This design is shown in Fig. 28. The ceramic seals are made to copper which, in the relatively thin sections used, has been found sufficiently ductile to make vacuum tight seals capable of withstanding all normal thermal shocks. (It will withstand alternate immersion in dry ice and acetone and then boiling water.)

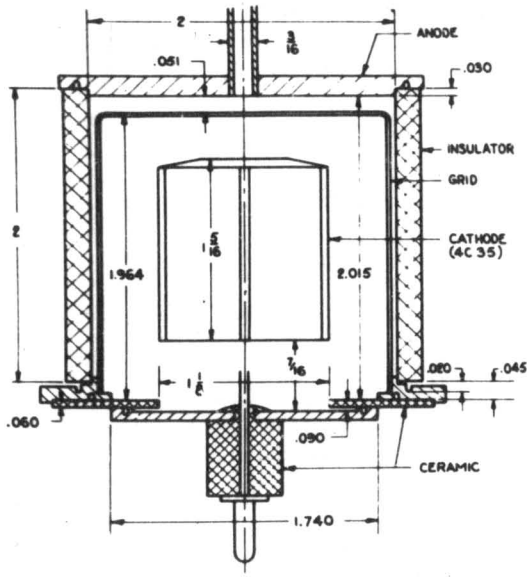

Fig. 27 Basic design for a tube assembly using a low temperature solder.

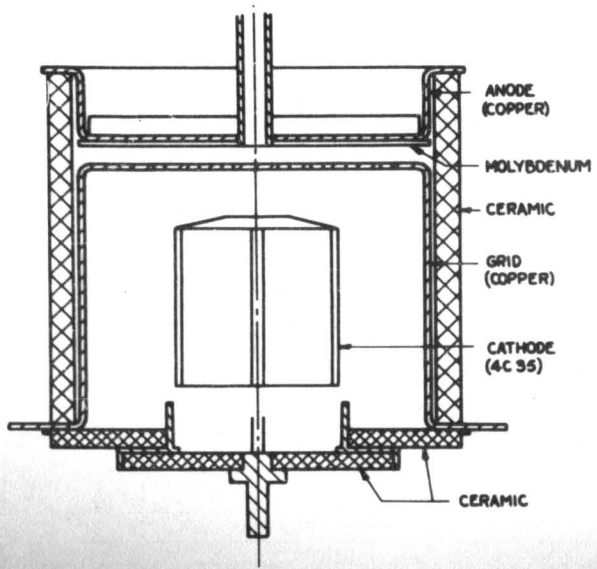

Fig. 28 Basic design for a ceramic-metal assembly using silver solder for final brazing.

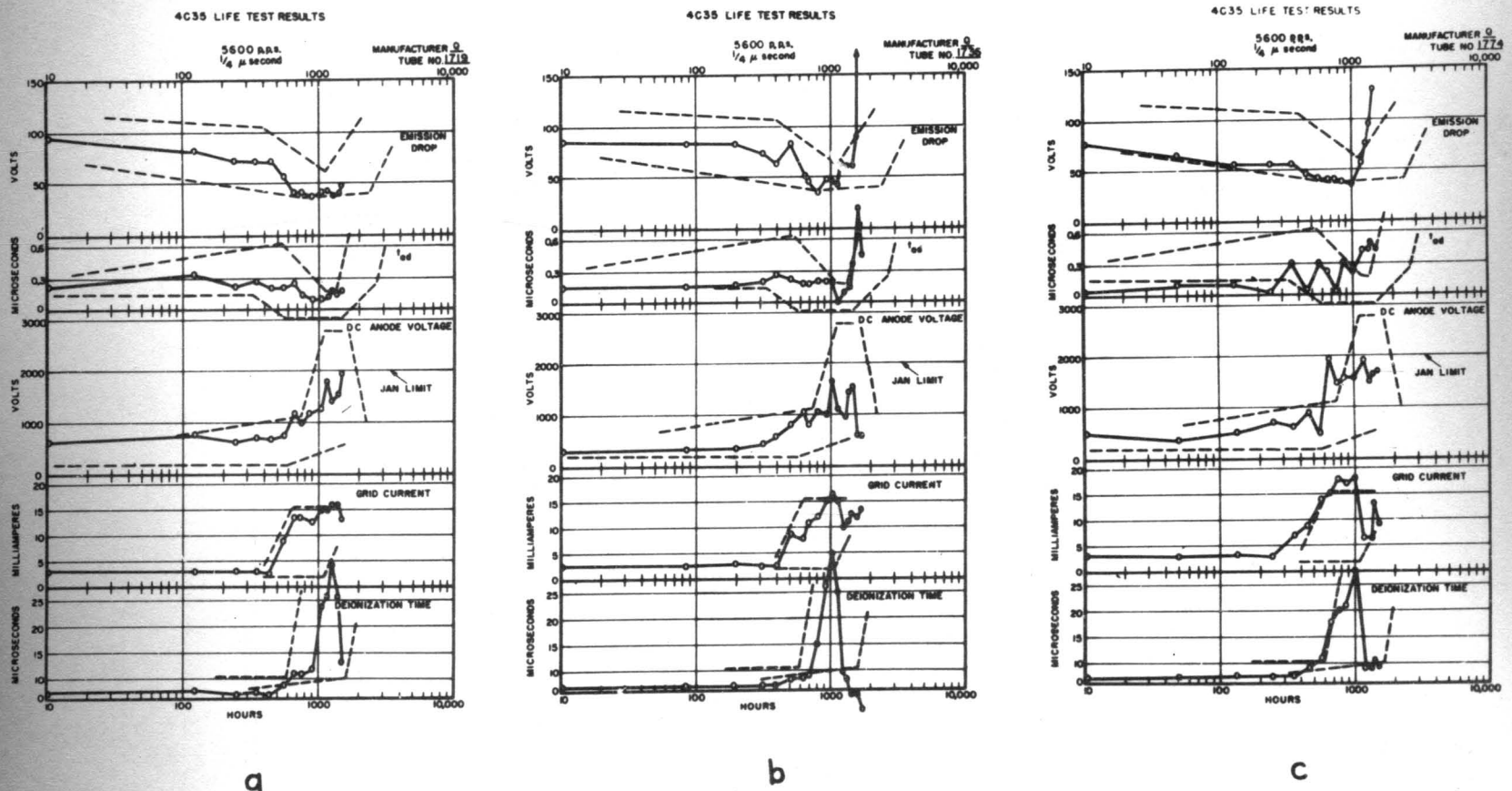

Fig. 29 (a - c) 4C35 life test results - 5600 pps - 1/4 microsecond i_h = 90 amps.
Dashed lines are envelopes of corresponding parameters under JAN conditions. Note tendency of grid emission to occur earlier in this test, and emission drop minimum to be deeper.

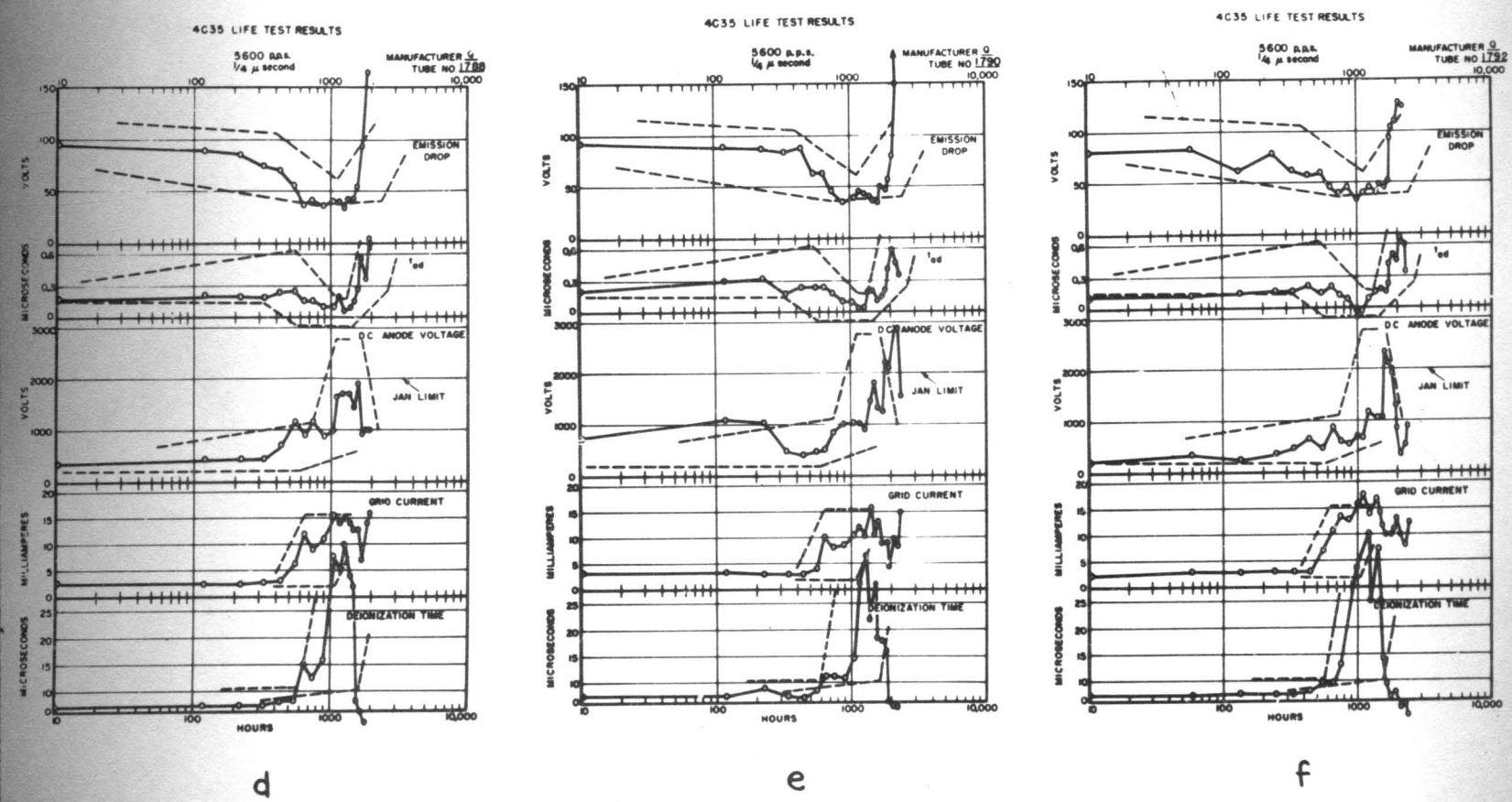

Fig. 29 (d - f) 4C35 life test results - 5600 pps - 1/4 microsecond i_h = 90 amps.
Dashed lines are envelopes of corresponding parameters under JAN conditions. Note tendency of grid emission to occur earlier in this test, and emission drop minimum to be deeper.

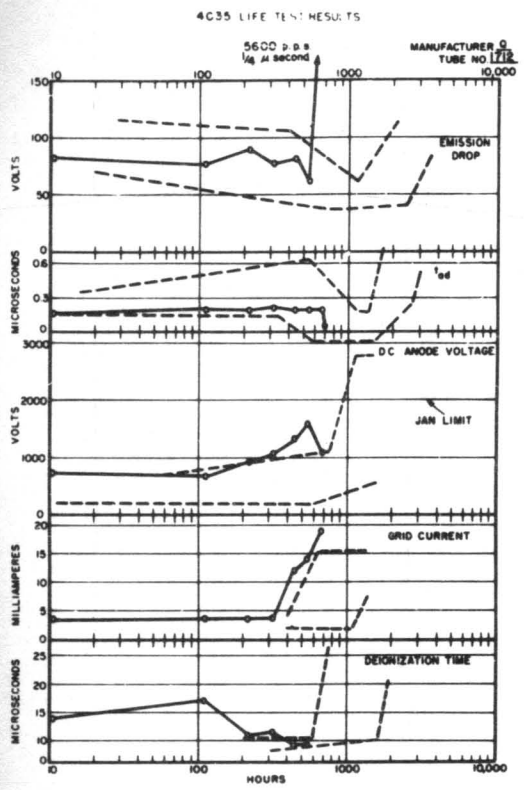

g

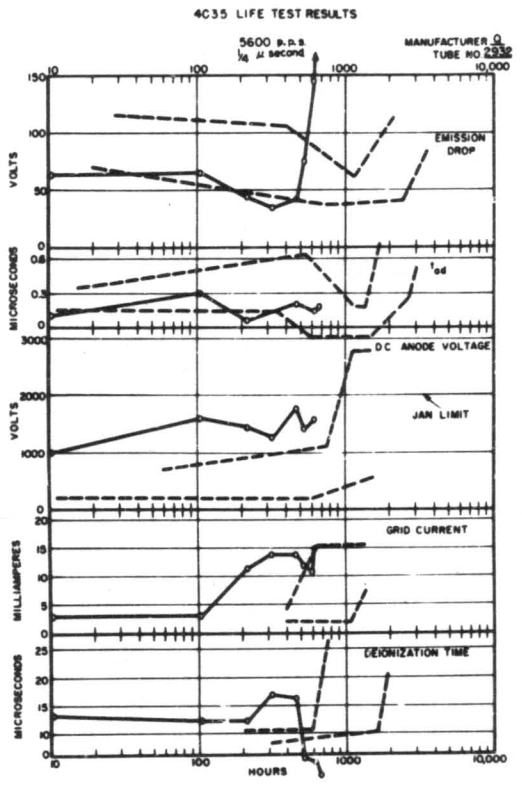

h

Fig. 29 (g, h) 4C35 life test results - 5600 pps - 1/4 microsecond i_h = 90 amps.
Dashed lines are envelopes of corresponding parameters under JAN conditions. Note tendency of grid emission to occur earlier in this test, and emission drop minimum to be deeper.

CONCLUSIONS

Experimental and theoretical work completed during this period has demonstrated that a hitherto unsuspected effect, the flow of a substantial reverse current for a few millimicroseconds at the end of the pulse, profoundly influences anode dissipation and tube life.

The inverse voltage appearing on the tube after conduction has ceased is fairly complex, if the load is inductive, even though the pulse network is a perfect transmission line. It consists of several identifiable parts as follows:

(a) The impedance mismatch voltage

$$\left\{\frac{R_L - Z_o}{R_L + Z_o}\right\} e_{pq}$$

(b) An additional voltage determined by the circuit inductance which increases the inverse. This voltage will appear periodically beginning approximately a pulse length after cessation of current flow and thereafter with a period which is exactly the pulse length. These maxima will be present even though the mismatch voltage is zero.

(c) A periodically recurring voltage which makes the inverse less than the mismatch inverse. This voltage is primarily determined by the current which flows in the reverse direction (collection of positive ion by the anode). In certain cases it is possible that this voltage will cause the inverse to swing positive for a short interval of time. This voltage also appears approxi-

mately one pulse length after current flow has ceased and thereafter with a period of precisely one pulse length.

(d) A very short spike of voltage which appears a few millimicroseconds after the end of the current pulse and which makes the inverse voltage greater than the mismatch inverse. This voltage is caused by the flow of reverse current in the circuit impedance. Measurement is difficult because of the extreme rapidity with which this spike appears and disappears. It evidently has frequency components ranging above 100 Mcs.

The power dissipated during the appearance of inverse voltage is all localized in the first 50 to 100 millimicroseconds, since the flow of reverse current is substantially over in that interval. All of this power is dissipated in the anode. The energy may easily be substantially greater than that dissipated during any other part of the conduction period.

These results have been corroborated by life tests run at high frequencies with various inverse voltages applied. Anode dissipation is substantially greater at the higher inverse voltages and life is appreciably shortened.

Analysis of tubes run at high inverse voltage shows severe erosion of the anode which has been traced entirely to the effect of bombardment by hydrogen ions. In the case of very high power tubes this bombardment can produce local melting of the molybdenum surface in addition to sputtering. It is probable, however, that sputtering is

not of itself a major cause of failure.

Life test results obtained on tubes run at high frequencies and appreciable inverse voltage indicate that the ultimate cause of failure is insufficient dissipation by the grid. There would apparently be little damage done by operating a hydrogen thyratron with red anode if the dissipation of the grid were sufficient to prevent buckling and grid emission.

PROGRAM FOR NEXT INTERVAL

1) Construct additional 1907 life test units.

2) Perform additional life tests to investigate the effect of inverse voltage.

3) Investigate a means of determining pressure by internal measurements on the hydrogen thyratron.

4) Investigate the mechanism of commutation and the anode dissipation resulting therefrom.

5) Determine the effect of external circuit values on power dissipated during breakdown and during inverse.

6) Measure recovery time as a function of reapplied voltage, inverse voltage, pulse current, and grid bias.

7) Assemble an experimental ceramic hydrogen thyratron.

PERSONNEL LIST

			Approximate Hours Spent on Contract the Sixth Period
Kenneth J. Germeshausen	-	Vice-President	150
Dr. Stuart T. Martin	-	Contract Associate	368
Dr. William P. Allis	-	Consultant	
Harold Bernstein	-	Engineer	535
Seymour Goldberg	-	Engineer	554
Daniel Riley	-	Engineer	554
James Stoms	-	Engineer	13
Technicians	-		1344
Drafting	-		230